THE ASTROPHYSICAL JOURNAL, 379:532–548, 1991 October 1

VACUUM ULTRAVIOLET IMAGERY OF THE VIRGO CLUSTER REGION. III. DIFFUSE FAR-ULTRAVIOLET RADIATION AT HIGH GALACTIC LATITUDES

TAKASHI ONAKA
Department of Astronomy, Faculty of Science, University of Tokyo, Bunkyo-ku, Tokyo 113, Japan
AND
KEIICHI KODAIRA
National Astronomical Observatory, Mitaka, Tokyo 181, Japan
Received 1990 November 19; accepted 1991 April 17

ABSTRACT

Far-ultraviolet radiation over a wide sky region of $-110° < l < 60°$ and $b > 60°$ was observed by a rocket-borne two-dimensional imager in the wavelength around 150 nm. The background far-ultraviolet radiation from the Virgo cluster region was also observed in the pointing phase of the same rocket experiment. Contributions from several components, such as airglows, faint stars, or molecular hydrogen emission, to the observed radiation were examined, and the diffuse far-ultraviolet background radiation at high Galactic latitudes was derived. The results showed a steep dependence of the background radiation on the Galactic latitude b, and the radiation flux in the region of $b > 70°$ and of $N(\mathrm{H\ I}) < 3 \times 10^{20}$ cm^{-2} to be 300–600 photons cm^{-2} s^{-1} Å^{-1} sr^{-1}. A clear correlation of the background radiation with the hydrogen column density N(H I) was obtained in the region of $b > 70°$. The correlation was confirmed by the background radiation in the Virgo cluster region, indicating that major part of the background radiation is Galactic origin. The observed steep dependence on b cannot be explained easily by simple models of light scattering by interstellar dust grains with uniform source distribution. We propose a model of light scattering by dust with anisotropically distributed far-ultraviolet stellar sources in the Galactic disk. Comparison of the model calculation with the observation indicates that, as for scattering properties of the interstellar dust grains, the albedo a is larger than 0.32 and the scattering phase asymmetry factor g is greater than 0.5. These results are in agreement with some theoretical predictions. The regression line of the observed flux versus N(H I) intercepts with the ordinate axis at 200 to 300 photons cm^{-2} s^{-1} Å^{-1} sr^{-1}, in which the Galactic isotropic component and the extragalactic component are involved. The difference in the background radiation between inside and outside the Virgo cluster was shown to be less than 2 photons cm^{-2} s^{-1} Å^{-1} sr^{-1}. This can set an upper limit to the decay light of neutrinos from the Virgo cluster, and a lower limit of about 6×10^{24} s to be lifetime of the heavy neutrinos of the mass around 15 eV c^{-2}, if the mass of the Virgo cluster derived from the X-ray observations is allocated to heavy neutrinos.

Subject headings: galaxies: clustering — interstellar: grains — neutrinos — ultraviolet: general

1. INTRODUCTION

The "sky background" in the far-ultraviolet (FUV) region is much lower than in the visual region (O'Connell 1987), and the observation of the diffuse FUV radiation may be "the holy grail" in the search for the intergalactic and extragalactic low surface brightness radiation (Paresce 1990). Several components from terrestrial airglow to extragalactic sources could contribute to the diffuse FUV background radiation (Paresce & Jakobsen 1980). There has been a considerable uncertainty about the magnitude of these individual sources. This situation has often hampered a simple, direct interpretation of the observation. There has also been remarkable disagreement in the extent of spatial variation and the magnitude of the diffuse FUV background radiation. A most recent review is found in Bowyer (1990).

Owing to latest experiments, however, the nature of the FUV diffuse background radiation has been revealed more clearly than before (Murthy et al. 1989, 1990; Fix, Craven, & Frank 1989; Martin & Bowyer 1990; Martin, Hurwitz, & Bowyer 1990; Hurwitz, Martin, & Bowyer 1990, hereafter HMB). The intensity level at high Galactic latitudes seems to be around a few hundreds photons cm^{-2} s^{-1} Å^{-1} sr^{-1} (hereafter called "continuum units" or CU). The extent of the spatial variation and the correlation with the H I column density are still controversial, but the point of the discrepancy has become much more restricted. The degree of the contributions from terrestrial airglow became easier to be estimated since the altitude dependence and the emission mechanisms have been spectroscopically studied to a large extent (Brune et al. 1978; Tennyson et al. 1986). The intensities of emission from molecular hydrogen and ionic species were detected in the diffuse FUV spectra, and the contribution to the diffuse continuum are now better understood than before (Martin & Bowyer 1990; Martin et al. 1990). Part of the discrepancy in early observational results of the FUV diffuse background radiation might have originated from the contamination by terrestrial airglow and stray light, the exclusion or different modeling of the effects of a stellar contribution, the difference in the absolute calibration, and the differences in the observed areas and spectral regions.

Several observations indicate the correlation of the diffuse FUV radiation with the neutral hydrogen column density N(H I) or the diffuse far-infrared (FIR) radiation, suggesting that the major part of the diffuse FUV radiation is the starlight scattered by interstellar dust grains (Paresce, McKee, & Bowyer 1980; Joubert et al. 1983; Jakobsen et al. 1984; Jakob-

sen, de Vries, & Paresce 1987; Fix et al. 1989; Lequeux 1990; HMB). However, there is still controversy in observational results of the diffuse FUV radiation, in particular, of its spatial variation (see § 4.2). If the starlight scattered by interstellar dust grains dominates in the observed diffuse FUV radiation, spatial variations are expected with the Galactic latitude and the local H I column density. The intensity and the spatial variation of the diffuse FUV radiation, therefore, provide information about the scattering properties of the interstellar dust particles (Jura 1979a, b; Witt 1989, 1990). The Galactic FIR diffuse radiation is thought to come from the thermal emission of the same interstellar grains which absorb the interstellar FUV to visual radiation. Correlations of the diffuse FUV radiation with the FIR radiation are also useful in the study of the absorption and scattering properties of the interstellar dust particles (Jakobsen et al. 1987).

The isotropic component in the diffuse background radiation is of great interest in connection to extragalactic sources, such as distant galaxies (Code & Welch 1982; Martin & Bowyer 1989). It has also been suggested that heavy neutrinos which may make a substantial contribution to the dark matter in the universe can be detected by the decay radiation in the FUV region (Cowsik & McClelland 1972; De Rujula & Glashow 1980). Searches of the decay light in massive objects, such as clusters of galaxies, are of particular interest, but attempts to detect the decay light from the massive neutrinos have so far been unsuccessful, only providing lower limits of the decay time of the massive neutrinos (Kimble, Bowyer, & Jakobsen 1981; Henry & Feldman 1981; Weller 1983; Holberg & Barber 1985; Murthy & Henry 1987).

In this paper, we present the observation of the diffuse FUV radiation obtained by a rocket-borne FUV two-dimensional imager (Onaka et al. 1989; hereafter Paper I). The experiment was primarily aimed at obtaining the total FUV fluxes from galaxies in the Virgo Cluster (Kodaira et al. 1990, hereafter Paper II). The observation of the diffuse radiation with a two-dimensional imager allowed to have a large field of view with feasible subtraction of stellar signals at expense of spectral information. The spectral observation is a useful means to separate the individual contributions, while photometric observations have an advantage to study the spatial variation over a wide sky area. Owing to the progresses in spectral observations as mentioned above, the contributions of the airglow and of the line and molecular emissions in the medium-band photometry can be estimated with reasonable accuracies. The observation of diffuse radiation with the imaging instrument, thus, should be regarded as a complemental means to the spectroscopic observation.

Two-dimensional imaging in the FUV region has been applied to the study of physical properties of dust grains in extended nebulosities (Carruthers & Opal 1977a, b; Bohlin et al. 1982). Recently, Martin & Bowyer (1989) obtained a two-dimensional image of the diffuse FUV background radiation in a region of low H I column density. They found fluctuations of 4% on a scale of 6′–12′ and identified them with the integrated light from distant galaxies.

The observational results of the present study can be divided into two sets. The first set was obtained while the rocket was in the acquisition phase. The observed area in this phase was in the region of $b > 60°$ and $-110° < l < 60°$. The second data set was taken in the pointing phase when the rocket was pointing to the Virgo Cluster. The two data sets enable us to study the spatial variation both over a wide area and in a local region, and to contribute resolution of the problems about the diffuse FUV radiation. In § 2, the procedures of the data reduction are described, while the observational results, in particular, the spatial variations with the H I column density and with the diffuse FIR flux are presented in § 3. They are discussed in § 4 in connection to models of the dust scattering and to the extragalactic component. A preliminary result of this study has been reported by Onaka (1990).

2. OBSERVATION AND DATA REDUCTION

The FUV imaging experiment GUV aboard an attitude-controlled sounding rocket S520–8 consisted of two identical telescopes, each of which looked at the sky 3° apart with a field of view of 4° in diameter (3.8×10^{-3} sr). One pixel size of the detector system corresponded to 4.9×10^{-7} sr. The spectral response peaked at 156 nm with the FWHM of 23 nm. Further details of the instrumentation and the calibration of the system as well as of the rocket flight were described in Paper I. In this section a brief summary of the observation and the data reduction is given in connection to the analysis of diffuse background radiation.

2.1. *Acquisition Phase*

The GUV system was powered on 117 s after the launch and the rocket was pointed at the target, the Virgo Cluster, at 250 s after the launch. Before the pointing, GUV observed the sky area around the Virgo Cluster (acquisition phase). The acquisition path, which had not been specified in advance, was as shown in Figure 1. One of the telescopes, GUV1, was installed on the rocket axis, while the other, GUV2, was placed 3° off the axis. Since the spinning motion of the rocket dominated in the acquisition phase, the trajectory of the center of the field of view of GUV2 figured an epicycle on the sky. In Figure 1, the H I column density deduced from the H I 21 cm observation (Helies 1975) is also indicated.

The signals were stored in the memory on board and telemetered to the ground every 2.52 s. Thus, a frame of the "picture" sampled the radiation from the varying area of the sky which the telescope scanned in 2.52 s. Each picture was divided into two parts to yield maximal spatial information with enough count rates, and the background signals were integrated for each part. Since the dominant motion of the field was the rotation along the rocket axis, the divisions were made as follows: for GUV1, the circular area enclosed by a circle with the radius of 1°.4 and the annular area outside the circle; and for GUV2, the fan-shaped area with the distance to the center of the GUV1 field of view less than 3°.2, and the remaining fan-shaped area. Each part has an almost equal size of the field of view (1.9×10^{-3} sr), and the number of photons collected in each part is typically over 1000 before the subtraction of discrete sources (see below). The size of the area which each part scanned depends on the position of the scan path, being $(5–10) \times 10^{-3}$ sr at the beginning of the scan and typically $(2–3) \times 10^{-3}$ sr. Any dependence on the size of the scanned area was not seen in the reduced data. The areas each part scanned partly overlapped with each other and a total of the sky area of about 0.2 sr was scanned in the acquisition phase.

Each picture was flat-fielded and calibrated absolutely by using the data taken at the laboratory prior to the flight. The absolute scale of GUV was found to be 80% of that of the 156.5 nm band of *TD-1* experiments (Paper I). The test at the laboratory and examination of the observed stellar signals did not

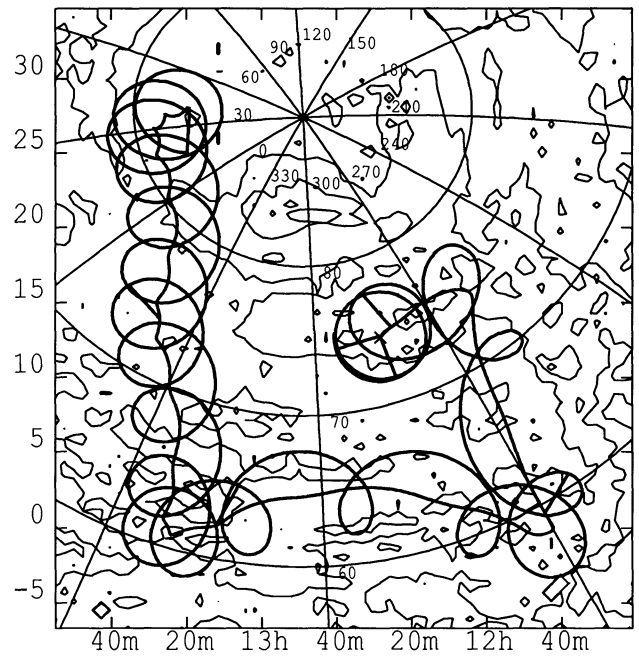

FIG. 1.—Area of the sky which the present experiment observed. The x-axis shows α(1950.0) (m), and the y-axis shows δ(1950.0) (deg). The trajectories of the telescope axes are indicated by thick lines: the epicycle one shows that of GUV2, which was placed 3° off the rocket axis, and the other that of GUV1 on the rocket axis. Thick straight lines connecting the two trajectories indicate the time interval of 10 s. The coordinates are equatorial with the Galactic coordinates being drawn in. The contours are the H I column density and the unit is 1×10^{20} cm^{-2}. The H I data were taken from Heiles (1975) with the estimated offset flux (4.5×10^{19} cm^{-2}) being subtracted (see text § 3.1).

indicate any significant change of the sensitivity with time after the power-on of the GUV instrument. The area where discrete sources contaminated were excluded in the integration of the signals. All stars whose spectral types are earlier than F9 or whose visual magnitudes are brighter than 7 mag in the SAO catalog were taken into account. Since the point spread function had an FWHM of 16′ at maximum (Paper II), the area of 30′ band along the trajectory of a discrete source was excluded. The sources in *TD-1* catalog (Thompson et al. 1978) and *ANS* (Wesselius et al. 1982) were all detected in GUV, and their trajectory areas were excluded. Areas contaminated by anonymous objects whose flux larger than 1×10^{-12} ergs cm^{-2} s^{-1} Å^{-1} at 156 nm and by overlapping objects (Paper I) were also excluded. Possible contributions from stellar objects fainter than the above flux will be discussed in § 4. Forty stars were detected in the acquisition phase (Paper I). A substantial fraction of the pictures were contaminated by the stellar signals. The parts, more than 85% of whose area were contaminated by the stellar signals, were excluded in the further analysis. A total of 142 parts in the acquisition phase were left for the analysis. The excluded parts were shown not to make any significant effect on the results discussed in this paper.

2.2. *Pointing Phase*

The data taken between 250 s and 431 s after the launch were stacked using the attitude data of the rocket to construct images of the Virgo Cluster (pointing phase). The data after 431 s from the launch were excluded because of the contamination of the airglow (see below). The data were smoothed by a Gaussian function in Paper II to enhance the accuracy in the position determination and the source detection. In the present analysis, the original stacked data without smoothing were used, while the position and source detections referred to Paper II. The area of 8.6×10^{-5} sr was integrated corresponding to the resolution of the H I data (see below). The areas which were contaminated by discrete sources, including anonymous objects, were excluded in the integration. The flux limit of the discrete sources whose areas were excluded was estimated to be about 8×10^{-15} ergs cm^{-2} s^{-1} Å^{-1}. Finally entry of 47 parts in the pointing phase were obtained and they covered an area of 4×10^{-3} sr in all.

2.3. *Subtraction of the Component Varying with the Altitude*

The data in the pointing phase showed a dependence on the altitude of the rocket in the downleg (Fig. 2). Since each telescope looked at almost the same sky area during this phase with the elevation angle of 60°, we attributed the observed variation to the terrestrial airglow.

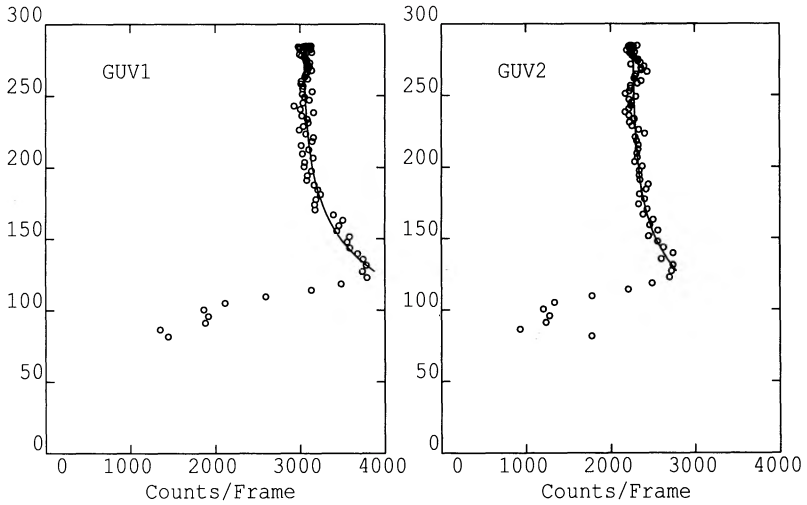

FIG. 2.—Count rates vs. the altitude of the rocket in the downleg. The data points were fitted with the exponential function with the scale high of 36 km (see eq. [1]).

In previous experiments with similar spectral response functions the resembling altitude variations were observed, and they were attributed to the NO emission (Jakobsen et al. 1984; Martin & Bowyer 1989). We fitted the variation by an exponential function following the previous researchers:

$$I = I_0 + I_{NO} \exp(-h/h_0), \quad (1)$$

where h is the altitude of the rocket, h_0 is the scale height of the NO emission, and I_0 is the constant component independent of the altitude. The parameters in the fitting were I_0, I_{NO}, and h_0. The best-fitted value of h_0 to the data given in Figure 2 was found to be 36 ± 2 km. This value of h_0 is in agreement with those obtained by Jakobsen et al. (1984) (30.3 km) and Martin & Bowyer (1989) (30.5 km). The observed altitude variation is also consistent with the data obtained by Tennyson et al. (1986) who investigated the line emission of NO at midnight in detail.

The data were corrected for the altitude dependent component by subtracting the exponential term of equation (1) from the observed count and by taking account of the dependence on the elevation angle of the GUV telescope expected for the optically thin emission. At the beginning of the acquisition phase the rocket already reached above 170 km and the contribution of the exponential term was less than 10% of the total signal and less than 5% in most cases. The data below 170 km in the pointing phase (the data taken after 431 s from the launch) were discarded to minimize the uncertainty of the correction. There may still remain airglow components left in the corrected data which do not show an apparent variation with the altitude. The data presented in the following are corrected only for the exponential term in equation (1), leaving the constant component of airglow uncorrected. The contribution from various uncorrected components will be discussed in § 4.

3. RESULTS

3.1. *Spatial Variation of the Diffuse FUV Background Radiation*

Figure 3 shows the plot of all the FUV data taken in the acquisition phase against the H I column density. The H I 21 cm data were taken from the Bell Laboratory survey (Stark et al. 1990), and the H I 21 cm line was assumed to be optically thin. The GUV scanned area of each part is typically spread over 5°, while the FWHM of beam of the H I observation is about 2°. The H I data within the area scanned by GUV were averaged to yield the corresponding H I column density in the picture part. The regression line is given by

$$I_{FUV}(\mathrm{CU}) = (37.7 \pm 12.0)\left[\frac{N(\mathrm{H\ I})}{10^{20}\ \mathrm{cm}^{-2}}\right] + (387.7 \pm 25.9), \quad (2)$$

where I_{FUV} is the diffuse FUV background intensity in CU and N(H I) is the H I column density. Hereafter the given errors of the slope and the intercept are 1 σ unless otherwise mentioned. The correlation coefficient is 0.21 and the correlation is weak. The data taken during the pointing phase were divided into four parts in the same way as in the acquisition phase for the sake of comparison. The average intensity of each part thus obtained for the pointing phase is also indicated by squares in Figure 3. Two data points largely deviating above the regression line are the ones around R.A. = 13^h24^m and $\delta = 0°.8$. In the vicinity of these points, there was the brightest star ζ Vir in the GUV observation. Although there is no apparent evidence,

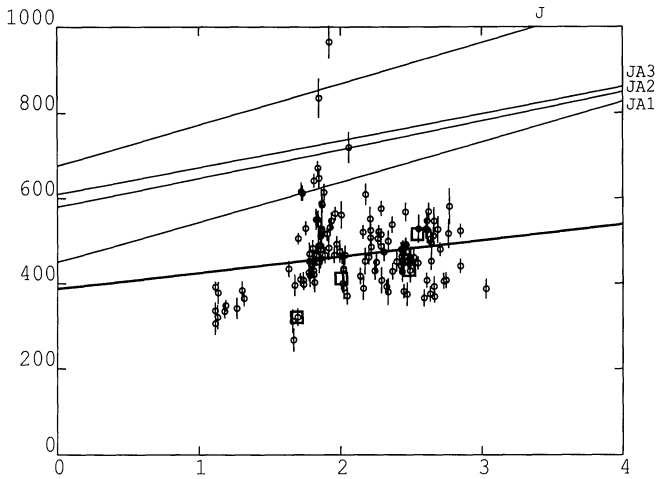

FIG. 3.—Diffuse FUV radiation (I_{FUV}) (photons cm^{-2} s^{-1} Å^{-1} sr^{-1}) observed in the acquisition phase is plotted against the H I column density, N(H I) (10^{20} cm^{-2}). Squares indicate the data taken during the pointing phase and reduced in the same way as in the acquisition phase. The regression line is shown by a thick line. Thin straight lines are those obtained by previous researchers; J: Joubert et al. (1983) 169 nm band data, JA1, JA2, and JA3: Jakobsen et al. (1984) 159 nm band data.

it cannot be ruled out that some instrumental scattered light or the distortion of the image on the edge of the detector system (ζ Vir was always located on the edges) might have contaminated the diffuse flux around this region. We have excluded these two points in the followings and in all the regression line analyses in this paper. In Figure 3, the relations obtained by Joubert et al. (1983) at 169 nm (denoted by "J") and Jakobsen et al. (1984) at 159 nm (JA1, JA2, and JA3) are also depicted. It is clear that the intensity level of the present data is lower and the regression line is less steeper than the previous experiments as far as Figure 3 is concerned.

The plot of the FUV data against the Galactic latitude b is shown in Figure 4 for the parts whose H I column density was between 1.8×10^{20} and 2.0×10^{20} cm^{-2}. Figure 4 indicates a systematic decrease of the diffuse FUV radiation with increasing b. To quantify the dependence, the data were fitted by a

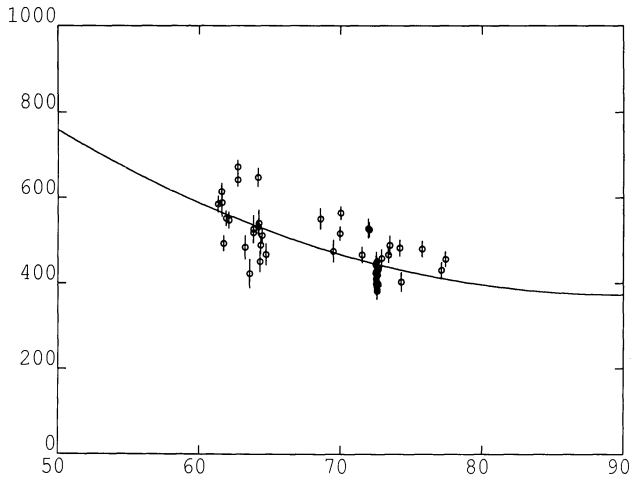

FIG. 4.—Diffuse FUV radiation (I_{FUV}) (photons cm^{-2} s^{-1} Å^{-1} sr^{-1}) with $1.8 \times 10^{20} < N(\mathrm{H\ I}) < 2.0 \times 10^{20}$ cm^{-2} is plotted against the Galactic latitude b. A best-fitted curve (eq. [3]) is also shown.

function of $(\sin b)^{1/2}$, which is a latitude dependence suggested for the scattering by dust particles in high Galactic latitudes by Jura (1979a). The least-square fit gives

$$I_{\rm FUV}({\rm CU}) = -(3098.9 \pm 390.0)(\sin b)^{1/2} + (3471.5 \pm 376.7), \quad (3)$$

with the correlation coefficient of -0.70. The scatter around the fitted curve in Figure 4 is larger than the observational errors, indicating that equation (3) does not have any other meaning than an indication of the global trend of the diffuse radiation with b.

The range of the H I column density in this analysis was restricted to eliminate the dependence on the column density. This range was selected because the data of this slice in N(H I) were spread over the widest latitude range and had the most points. Other slices in N(H I) were also examined. The data of N(H I) $< 1.4 \times 10^{20}$ cm^{-2} or of N(H I) $> 2.2 \times 10^{20}$ cm^{-2} are located in a small range of the latitude and do not give any meaningful information on the dependence on the latitude. Slices of 1.6×10^{20} cm$^{-2} < N$(H I) $< 1.8 \times 10^{20}$cm^{-2} and 2.0×10^{20} cm$^{-2} < N$(H I) $< 2.2 \times 10^{20}$ cm^{-2} have a less number of data points or are spread over a smaller range of the latitude than that shown in Figure 4, but both indicate a similar trend of the decrease with b. In fact, the least-square fit of all data points of 1.6×10^{20} cm$^{-2} < N$(H I) $< 2.2 \times 10^{20}$ cm^{-2} by the function of $(\sin b)^{1/2}$ gives the slope of (-3361.2 ± 411.0) and the intercept of (3671.0 ± 398.4), which are consistent with equation (3), although the plot against b shows a more scatter than Figure 4. The results derived from the adopted sliced data are thus considered to represent typical dependence of the diffuse radiation on b.

In order to suppress the effect of the latitude dependence, only the data for $b > 70°$ are plotted against the H I column density in Figure 5. The regression line is given by

$$I_{\rm FUV}({\rm CU}) = (78.1 \pm 7.2)\left[\frac{N({\rm H\ I})}{10^{20}\ {\rm cm}^{-2}}\right] + (278.7 \pm 16.2) \quad (4)$$

with the correlation coefficient of 0.60. The correlation becomes more obvious and the slope of the line becomes steeper than those in Figure 3. If we further restrict the range of the data to $b > 75°$, the correlation coefficient turns to 0.83 and the slope turns out to be 97.2 ± 4.6 in the same units.

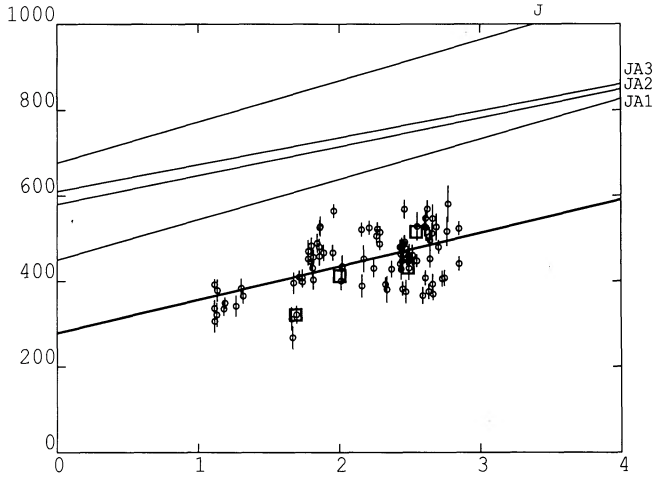

FIG. 5.—Same as Fig. 3, except that only the data with $b > 70°$ are plotted

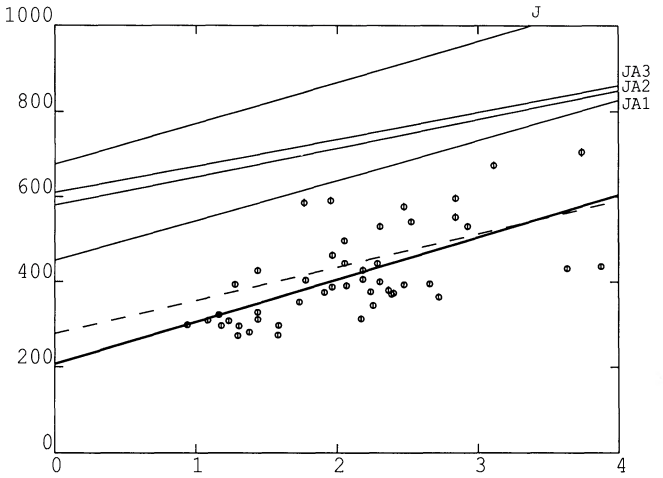

FIG. 6.—Same as Fig. 3 for the pointing phase data. Broken line indicates the regression line obtained in Fig. 5.

The data of N(H I) $\sim$ (1–1.2) $\times 10^{20}$ cm^{-2} were taken at the area of the beginning of the GUV observation (R.A. $\sim 13^{\rm h}30^{\rm m}$ and $\delta \sim 30°$; see Fig. 1). Those at N(H I) $\sim$ (1.6–1.8) $\times 10^{20}$ cm^{-2} are for the area at R.A. $\sim 13^{\rm h}30^{\rm m}$ and $\delta \sim 10°$. The data of N(H I) $\sim$ (2–3) $\times 10^{20}$ cm^{-2} are mostly concentrated in the area of the trajectory right before the target. The data obtained in the pointing phase (*squares*) are consistent with those in Figure 5. The points of the lowest N(H I) of the pointing phase, which is the most southern part of GUV2 image, is slightly off the regression line, but the deviation is within 3 σ. It seems thus to be justified that the correlation in Figure 5 is of global nature secured on the basis of the data taken over a widely spread area of $b > 70°$.

In Figure 6, the data taken during the pointing phase are plotted against the H I data. The corresponding H I data are taken from the Berkeley survey rather than the Bell Laboratory data mainly because of the appropriate spatial resolution of the former survey of HPBW = 0°.6 (Heiles 1975). Thus the corresponding FUV data were obtained by averaging over the area of the H I data resolution. The H I data of the Berkeley survey may be subject to the stray radiation (Heiles, Stark, & Kulkarni 1981), while the Bell Lab survey is thought to be free from it. We checked the correlation between these two data sets within the present observation area. We confirmed the linearity and found the offset value of $(4.5 \pm 2.2) \times 10^{19}$ cm^{-2}, which was in good agreement with the reported value (Heiles et al. 1981). We subtract the offset of 4.5×10^{19} cm^{-2} from all the Berkeley H I data we use in this study.

The regression line in Figure 6 is given by

$$I_{\rm FUV}({\rm CU}) = (99.3 \pm 17.8)\left[\frac{N({\rm H\ I})}{10^{20}\ {\rm cm}^{-2}}\right] + (207.1 \pm 39.3), \quad (5)$$

and the correlation coefficient is 0.64. This is slightly steeper than that in Figure 5, which is indicated by a broken line in Figure 6. The regression line analysis for the acquisition phase data with $b > 75°$ gives a compatible result. The standard deviation increases only 3% if we use the coefficients given in equation (4). Thus we cannot rule out the conclusion that the dependence on the H I column density is the same both for the data in the acquisition phase and the data in the pointing phase with the significance level of 25%. The correction of the

offset in the H I data has an effect of the change in the intercept by about 45 CU. There is an appreciable scatter of the data seen around the regression line. In the calibration at the laboratory the beam of about 0°.6, which is the same size of the data part in the present analysis, was used to measure the spatial variation of the detector sensitivity. Furthermore, the final pictures were obtained by stacking the data while the telescope was drifting over 1°. The spatial variation of the sensitivity must be smeared out over the drifted area. A total error in the measurement of the spatial variation of the instrumental sensitivity was estimated to be less than 10%, and the scatter in Figure 6 is larger than this experimental error.

3.2. *Local Features*

In the area scanned during the acquisition phase, some IR-excess cirrus clouds cataloged by Désert, Bazell, & Boulanger (1988) crossed the GUV field of view. We have checked the excess FUV flux at the corresponding positions in the same manner as employed in Paper I. The cloud C488 (the designation refers to Désert et al. 1988) was only briefly observed by GUV2, and no appreciable increment over 3×10^{-12} ergs cm^{-2} s^{-1} Å^{-1} was detected. The cloud C400 crossed the GUV2 field of view, but SAO 138252 overlapped and no information could be derived for the cloud. The clouds C363 and C364 overlapped with each other and were observed by GUV2. We found a marginal excess flux of $(1.2 \pm 0.6) \times 10^{-12}$ ergs cm^{-2} s^{-1} Å^{-1}. Since they were observed only once by GUV2, the detection should be confirmed by further observations.

We have also checked the area where Giovanelli & Haynes (1989) recently found a peculiar H I cloud. Unfortunately, the area was contaminated by stellar signals and only an upper limit of 3×10^{-12} ergs cm^{-2} s^{-1} Å^{-1} could be placed.

3.3. *Correlation with the Far-Infrared Radiation*

The diffuse FIR radiation was obtained from the *IRAS* skymap data (*IRAS* Explanatory Supplement 1986). The observed area was close to the ecliptic plane. Even at 60 μm, the contribution from the thermal emission from the zodiacal solid particles was dominating in the FIR radiation in the GUV observation field. Thus we used only the 100 μm data in the present correlation study. The zodiacal emission at 100 μm was estimated by a combination of the zodiacal emissions at 12, 25, and 60 μm according to Cox & Leene (1987). The data of the skymap were regridded to the ecliptic coordinates with the resolution of 1°, and the data of the area of interest, $150° < \lambda < 220°$ and $-15° < \beta < +50°$, were extracted, where λ and β are the ecliptic longitude and latitude, respectively. The diffuse smooth components in the three *IRAS* bands are assumed to be all attributed to the zodiacal emission. The extracted data are fitted by a summation of a skewed exponential function and a Gaussian function for each λ;

$$f_\nu = \exp(-A\beta^4 - B\beta^3 - C\beta^2 - D\beta - E) + \begin{cases} 0 & \text{for } |\beta| \geq 5°; \\ \exp(-F\beta^2 - G\beta - H) & \text{for } |\beta| < 5°, \end{cases} \quad (6)$$

where A, B, C, D, E, F, G, and H are the parameters in the fitting. The first five parameters were determined from the data for $|\beta| \geq 5°$ and the latter three were derived from the further fitting of the residual flux for $|\beta| < 5°$. We found that the skewed profile is necessary to describe the asymmetry of the observed profile, and an additional Gaussian was required to make a fine fitting in the vicinity of the ecliptic plane. We made a linear combination of the fitted functions of the three band fluxes as a model of the zodiacal emission at 100 μm and subtracted it from the 100 μm data. The coefficients of the combination were taken from Cox & Leene (1987). The accuracy of the correction was estimated to be about 1 MJy sr^{-1}. We also tried a model of a simple multiplication of the 60 μm flux according to Boulanger & Pérault (1988), but no significant difference between the two cases was seen in the final data.

As already demonstrated by previous researchers (e.g., Boulanger & Pérault 1988), the diffuse FIR flux correlates with the H I column density. We have examined the correlation of the derived data and found that the slope with the H I column density is in good agreement with that obtained by Boulanger & Pérault (1988), but that the zero level is different by about 1 MJy sr^{-1}. The zero level of the *IRAS* data has the uncertainty of the same order (Boulanger & Pérault 1988). In the following we do not take account of the offset level of the IR data, but discuss only the slope of the correlation. The slope is not affected by the method of the zodiacal emission correction.

The diffuse FIR radiation corresponding to each part in the acquisition phase was obtained by the same manner as done for the H I data. The correlation of the present FUV data in the acquisition phase for $b > 70°$ with the 100 μm flux thus obtained is shown in Figure 7. The regression line is given by

$$I_{\rm FUV}({\rm CU}) = (73.3 \pm 7.7)\left[\frac{f_\nu(100\ \mu{\rm m})}{\rm MJy\ sr^{-1}}\right] + (247.0 \pm 22.0)\,. \quad (7)$$

The correlation coefficient was 0.56. The correlation of FUV with FIR diffuse radiation found by Jakobsen et al. (1987) based on the FUV data of Jakobsen et al. (1984) was also shown by a thin line in Figure 7 with the intercept being adjusted. The difference from the present data is small as long as the slope is concerned. If $I_{\rm FUV}$ is taken as an independent variable, we obtain the slope of $(4.3 \pm 0.5) \times 10^{-3}$ MJy sr^{-1} CU^{-1}, which is consistent with the value derived by HMB.

4. DISCUSSION

We will discuss the spatial variation of the observed diffuse FUV background radiation in connection to the dust scattering light, and the isotropic component to the extragalactic

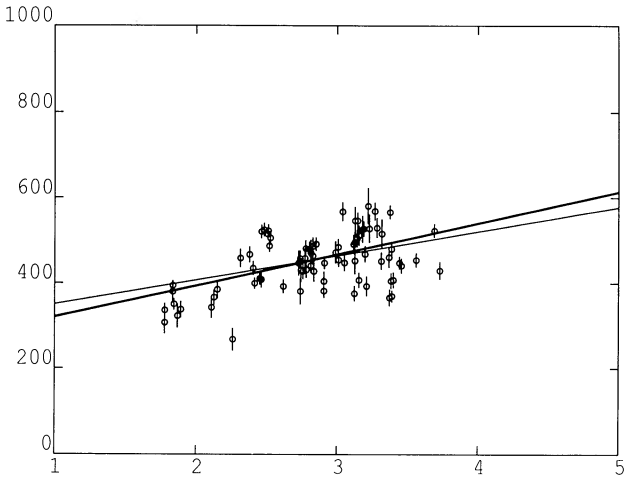

FIG. 7.—Diffuse FUV radiation ($I_{\rm FUV}$) (photons cm^{-2} s^{-1} Å^{-1} sr^{-1}) vs. the FIR radiation (f_ν) at 100 μm (MJy sr^{-1}) for the acquisition phase data. Thick line shows the regression line, while the thin line indicates the slope obtained by Jakobsen et al. (1987). The offset was adjusted for the thin line.

TABLE 1

ESTIMATES OF UNCORRECTED COMPONENTS IN GUV OBSERVATION

Component	Estimated Flux (CU)	Upper Limit (CU)	Comments
Dark current	23	25	GUV1
	35	40	GUV2
Airglow	6	36	dependence on the elevation angle <13 CU
Zodiacal light	0	1	
Faint stars	41	52	the acquisition phase
	21	27	the pointing phase
H_2 emission	43	43	correlated with N(H I)
Line emissions	17	33	anticorrelated with N(H I)
Ionized hydrogen	30	50	correlation with $b < 8$ CU ($60° < b < 80°$)

sources. Before proceeding to it, contributions from other potential sources, which have not yet been taken into account in the present data reduction, are examined in § 4.1. The discrepancies among previous observations are briefly reviewed in § 4.2.

4.1. *Potential Sources Contributing to the Diffuse FUV Radiation*

A summary of this subsection is given in Table 1, where probable values and upper limits of individual components are listed. Most probable values are still upper limits, but we may regard them as reasonable estimates in the further analyses. The certainty of each estimate can be inferred from the following discussion.

4.1.1. *Instrumental Dark Current*

The dark current was measured at the laboratory, its count rate being found to correspond to 12 CU on average without a noticeable dependence on the position of the detector. In flight we did not have a dark shutter to check the dark current. To make an estimate of the dark current in flight, we measured the count rate at the position just outside the edges of the field of view which were blocked by the frames of the microchannel plates. These data indicated that the dark currents corresponded to 23 ± 2 CU GUV1 and 35 ± 5 CU for GUV2.

4.1.2. *Residual Terrestrial Airglow*

Although we have corrected the component varying with the altitude (§ 2.3), there still remain possible constant components of terrestrial airglow in the corrected data. Tennyson et al. (1986, 1988) indicated that NO 1909 Å $\delta(0,0)$ emission remains even above 250 km. The intensity at 250 km was about one-fifth of that at 170 km in their observation. If the component varying with the altitude is attributed to NO 1909 Å emission, the observed intensity of the component is about 1.1 R at 170 km and 0.1 R at 250 km for the elevation angle of 60°. The "uncorrected" residual intensity, which has not been included in the exponential term equation (1), is, then, estimated to be 0.15 R. This corresponds to 6 CU.

The experiment by Tennyson et al. (1986, 1988) was made when the solar activity was high, while the solar activity was rather low at the time of the present observation. The NO emission is optically thin chemiluminescence, and its intensity is determined by the column densities of atomic oxygen and nitrogen. At low solar activity the atomic oxygen is supposed to be more confined (Jaccia 1977) and the atomic nitrogen density peaks at lower altitude (about 160 km compared to 200 km) (Rusch & Sharp 1981) than at high solar activity. The residual intensity from NO 1909 Å emission of 0.15 R thus estimated is certainly an upper limit. In the fitting of equation (1), the standard deviation was 9.4 CU. We conclude that the residual flux of NO 1909 Å is less than 16 CU in the data corrected only for the exponential term.

The O I 1356 Å line emission could also affect the present observation. Since we used a BaF_2 window to cut the line emission, only an upper limit of the sensitivity was measured at 135.6 nm in the laboratory. The O I 1356 Å line emission is well described by a model calculation, given the altitude density profiles of the electron and the oxygen atom (Brune et al. 1978; Onaka et al. 1985). The electron density was estimated from the ionospheric data (Ionospheric Data in Japan 1987), such that the maximum density n_{max} of 1.0×10^5 cm^{-3} occurred at $h_{max} = 300$ km at the present observation time. This is very similar to the conditions at the observation by Brune et al. (1978) ($n_{max} = 1.89 \times 10^5$ cm^{-3} and $h_{max} = 286$ km), who reported the intensity below 260 km is about 0.5 R for the elevation angle of 50°. The radiative recombination is thought to be a major emission mechanism for O I 1356 Å emission with 25% contribution from the mutual neutralization (Brune et al. 1978). Since the line is optically thin, the intensity below h_{max} can be scaled roughly by n^2_{max}. We estimated the intensity of O I 1356 Å emission at the present observation time to be 0.2 R for the elevation angle of 60° according to these data. This gives an upper limit of the contribution of 7 CU.

Since both the lines are optically thin emission and the lowest elevation angle we observed was 35°, the contribution of the airglow to the constant component did not exceed 36 CU for all the data and were less than 23 CU for $b > 75°$. Potential variation of the constant component due to the dependence on the elevation angle would be less than 13 CU.

4.1.3. *Zodiacal Light*

Previous observations of the zodiacal light in the FUV region were in considerable disagreement (a latest review is given in Tennyson et al. 1988). Recent studies in the wavelength range of 165 to 285 nm, however, indicated that the contribution to the diffuse background became appreciable in the wavelengths longer than 200 nm but was negligible below 200 nm (Tennyson et al. 1988; Murthy et al. 1990). Most recently, Lillie (1990) made detailed analysis on the zodiacal light below 300 nm, finding some increase in color below 200 nm. According to his results, we estimated the contribution from the zodiacal light to the GUV band to be less than 1 CU.

We conclude that the zodiacal light is not important in the spectral range of the present observation.

4.1.4. *Faint Stars*

In the procedure of the exclusion of the stellar signals in the acquisition phase, all stars of spectral types earlier than F9 and all stars brighter than 7 mag in the SAO catalog were taken into account (§ 2.1). The SAO catalog is considered to be complete to 8 mag, and stars contributing to the present spectral range are mostly A-type stars (Jakobsen et al. 1984). We estimated as a conservative upper limit that stars with $m_V > 6.5$ may have not been corrected in the procedure. The number of stars fainter than $m_V = 6.5$ mag around $b \sim 70°$ was estimated according to Allen (1973) with $m_{pg} - m_V = 1.0$. We obtained the visual surface brightness of 6.0 mag deg^{-2} as a contribution from faint stars. We assume that the color of the background stars in the high Galactic latitude can be represented by that of metal-poor elliptical galaxies. From Paper II we obtain $\log [f(150\text{ nm})/f(550\text{ nm})] = -1.86$ (NGC 4472) or -2.10 (NGC 4374). We finally estimated the contribution from faint stars to be 41 ± 11 CU. This is in good agreement with the estimate (55 CU) for a similar spectral response experiment given by Jakobsen et al. (1984), who used a different method in the estimation. HMB examined the contribution from faint stars in another way and obtained an upper limit of about 60 CU for $b > 45°$ with the threshold of $m_V = 7.5$ mag, which is also in agreement with the present estimate.

The fluctuation of the contribution from background stars was estimated according to the method of Jakobsen et al. (1984), being 10 CU for the field of view of 1.9×10^{-3} sr. We conclude an upper limit of the contribution from faint stars to be 52 CU in the acquisition phase data. If the faint stars are distributed in the disk, the dependence of the faint star contribution on the Galactic latitude will be given by cosec b. This gives the change of the faint star contribution from $b = 60°$ to $b = 80°$ as 7 CU. This is an upper limit of the change since some bright stars are distributed rather isotropically and they should show no dependence on b. The range of the variation with b seen in Figure 4 is more than 100 CU and cannot be attributed to the variation of the faint star contribution.

In the pointing phase, the limiting magnitude of excluded sources is much fainter than in the acquisition phase. The estimated value of the limiting flux of 8×10^{-15} ergs cm^{-2} s^{-1} Å^{-1} indicates $m_V = 10$ mag for an A5 star (Wesselius et al. 1980). If we assume all stars brighter than $m_V = 10$ mag are excluded in the pointing phase data, the same analysis as above indicates that the remaining contribution from faint sources is 21 ± 6 CU. Since stars brighter than $m_V = 10$ mag and later than A5 are not taken into account in this discussion, the value may be a lower limit. The difference of the faint stars' contribution between the acquisition phase data and the pointing phase data is, therefore, less than 25 CU.

The fluctuation estimated in the same way as above becomes large for the pointing phase since the field of view is small. However, the upper limit for the exclusion of discrete sources for a typical image size (16′ × 8.′2) (Paper II) corresponds to 70 CU for 8.6×10^{-5} sr. Fluctuations larger than this value could be identified with discrete sources and the data were excluded.

As pointed out by HMB, it is difficult to evaluate the uncertainty in these estimates. However, because estimates by different methods agree with each other to a reasonable extent, and because the estimates were made on the conservative assumptions, the values should be reasonable upper limits.

4.1.5. *Molecular Hydrogen Emission*

Duley & Williams (1980) suggested a possible contribution from the fluorescence emission of interstellar molecular hydrogen to the diffuse FUV background radiation. Absorption by the interstellar H_2 in the Lynman and Werner bands is followed by emission, leaving the molecule in some vibrational level v'' of the ground electronic state. If $v'' > 14$, the vibration level belongs to the vibrational continuum, and the molecule dissociates. Since this is the main destruction mechanism of the interstellar H_2, we can estimate the intensity of the fluorescence emission assuming the statistical equilibrium.

Jakobsen (1982) showed that the emission intensity observed by a wide-band photometer can be written as

$$I_{\rm FUV} = \frac{R n_{\rm H} N({\rm H\ I})}{4\pi \Delta\lambda}, \tag{8}$$

where R is the formation rate of molecular hydrogen, $n_{\rm H}$ the total hydrogen number density, N(H I) the H I column density, and $\Delta\lambda$ the effective band width of the observation for the H_2 band emission. As representative values, $R \sim 3 \times 10^{-17}$ cm^3 s^{-1} (Jura 1975) and $n_{\rm H} \sim 25$ cm^{-3} are often used. The effective band width $\Delta\lambda$ was calculated by convolving the line intensities calculated by Sternberg (1989) and the continuum intensity (Duley & Williams 1980) with the instrument sensitivity curve (Paper I), being 23.5 nm. The relative intensity of line emissions does not depend strongly on the environmental parameters (Sternberg 1989), thus the result is insensitive to the choice of the physical conditions of the observed area. We obtained for the present observation,

$$I_{\rm FUV}({\rm CU}) = 25\left(\frac{n_{\rm H}}{25\text{ cm}^{-3}}\right)\left[\frac{N({\rm H\ I})}{10^{20}\text{ cm}^{-2}}\right]. \tag{9}$$

Since the intensity is predicted to correlate with N(H I), part of the correlation seen in Figures 3 and 5 may be attributed to emission from molecular hydrogen (<20%).

A most recent study by Martin et al. (1990) detected the H_2 emission in the diffuse FUV radiation for the first time. According to their data, an upper limit of the emission intensity for regions of $N({\rm H\ I}) < 3 \times 10^{20}$ cm^{-2}, where most present data points are situated, is 1.3×10^4 photons cm^{-2} s^{-1} sr^{-1}, which is 43 CU in the GUV system. This is slightly smaller than the prediction of equation (3) for $n_{\rm H} = 25$ cm^{-3}. Thus, equation (3) is assumed to provide a reasonable upper limit of H_2 emission intensity to the continuum radiation. Martin et al. (1990) indicated that the contribution is less than 30% relative to the continuum in the 140–185 nm region.

4.1.6. *Line Emission from Hot Plasma*

Feldman, Brune, & Henry (1981) reported a possible detection of line emissions in the spectrum of the diffuse FUV radiation at a high Galactic region. Murthy et al. (1989), however, could not confirm the line emission in the nearby region, providing upper limits of the line intensities.

Lately, Martin & Bowyer (1990) reported a firm detection of the line emissions whose intensities were consistent with the upper limits given by Murthy et al. (1989). One of their targets (target 8 in Martin & Bowyer 1990) was located in the vicinity of the present observation area ($l = 334°$–$335°$; $b = 74°$–$82°$). According to the reported intensities at target 8, we estimated a total contribution from the line emissions in the GUV observations to be 17 ± 10 CU. At the region with the lowest H I column density [target 1; $N({\rm H\ I}) = 1 \times 10^{20}$ cm^{-2}] an upper

limit of the contribution from the line emissions was estimated to be 33 CU. Martin & Bowyer (1990) indicated an anti-correlation of the intensity with N(H I). If the line emissions are assumed to be negligible at N(H I) = 10^{21} cm^{-2} as a conservative estimate, we obtain a possible slope of the correlation of $-3.6 \times [N(\text{H I})/10^{20}\ \text{cm}^{-2}]$. This slope is one order of magnitude less than that found in Figure 3. We conclude that the contribution of line emission in the present experiment may be less than 33 CU. The effect on the slope of the regression line is less than 10%.

4.1.7. *Continuum Emission from Ionized Medium*

Deharveng, Joubert, & Barge (1982) examined the two-photon emission from the warm ionized medium and discussed its contribution to the diffuse background radiation. Reynolds (1990) showed that the total continuum intensity from the ionized interstellar hydrogen in the FUV is about 60 CU per 1 R of Hα line emission. According to the observation by Reynolds (1984), the intensity of the diffuse Hα emission generally decreases with increasing $|b|$ in a manner consistent with 1 R cosec $|b|$ for $|b| > 5°$, while a trend of the low intensity of 0.6 cosec $|b|$ R is suggested for high latitudes ($|b| > 60°$). The trend of the low intensity may be a result of the local fluctuation subjected to the undersampling of the sky (Reynolds 1984). We estimate that the contribution to the FUV continuum radiation from the ionized interstellar hydrogen is 50 CU at most and the most probable value is about 30 CU. The variation of this component between $b = 60°$ and $b = 80°$ is expected to be less than 8 CU and thus cannot be a major source to the observed variation of the background radiation shown in Figure 4.

4.2. *Observations of the Diffuse FUV Background Radiation*

There have been remarkable disagreements in the extent of *spatial variation* and in the magnitude of the diffuse FUV background radiation. A review of early observations was given by Paresce & Jakobsen (1980). At low to medium Galactic latitudes ($|b| < 60°$), the systematic spatial variation of the diffuse FUV radiation with the latitude was reported by several researchers (Hayakawa, Yamashita, & Yoshioka 1969; Lillie & Witt 1976; Morgan, Nandy, & Thompson 1978; Zvereva et al. 1982; Fix et al. 1989). The correlation with the H I column density was indicated in several observations at medium to high Galactic latitudes (mostly $|b| > 30°$) (Lillie & Witt 1976; Paresce et al. 1980; Joubert et al. 1983; Jakobsen et al. 1984; Fix et al. 1989). HMB indicated a clear correlation with the H I column density over a wide Galactic latitude range ($-39° < b < +88°$) as well as a variation with b. These variations are often interpreted in terms of the dust scattering, or sometimes in terms of the emission from hot gas (Severny & Zvereva 1983). The patchy nature of the FUV background radiation was suggested in an experiment (Paresce et al. 1979), while the presence of regions of excess FUV radiation was pointed out by other experiment (Joubert et al. 1983).

On the other hand, several observations at medium to high Galactic latitudes, including the Galactic pole regions, did not detect any spatial variation in the diffuse FUV background radiation (Henry et al. 1978a, b; Pitz et al. 1979; Anderson et al. 1979; Anderson, Henry, & Fastie 1982). A recent experiment on board a Space Shuttle indicated a spatial variation in the low to high Galactic latitudes, but did not show any systematic correlation with H I column density (Murthy et al. 1989, 1990). The other experiment aboard the same Space Shuttle, however, indicated a clear dependence of the FUV background radiation on N(H I) and b (HMB). Thus, spatial variation of the diffuse FUV radiation has so far been confirmed to some extent by several experiments, but its *systematic* variation with the Galactic latitude and the H I column density is still controversial.

The present results indicate that a steep spatial variation of the diffuse FUV radiation with the Galactic latitude (Fig. 4), which is consistent with one of the latest observations by Fix et al. (1989). In addition, we found that if we select the data at high Galactic regions ($b > 70°$), a correlation with N(H I) is clearly seen (Fig. 5). This correlation is further supported by the data for the limited area obtained in the pointing phase, which are supposed not to be affected by the large scale variation (Fig. 6). The slope of the correlation obtained in the present experiment is consistent with two recent observational results (Lequeux 1990; HMB).

There has been an intense interest in *the intensity level* of the diffuse FUV background radiation at high Galactic latitude regions or the intensity of the isotropic component in connection to the radiation originating from extragalactic sources. The intensity level of the isotropic component may depend sensitively on the estimate of contribution of the Galactic components. The slope of the regression line with N(H I) as well as the absolute intensity level could play a key role in this kind of analysis. There still exists some disagreement in the intensity level of the diffuse FUV radiation at high Galactic latitude region, but most recent experiments indicated the intensity of a range 300–500 CU for $|b| > 60°$. A brief summary of the previous observations in this concern is given in Table 2, in which the flux level at low neutral hydrogen column density [N(H I) < 3×10^{20} cm^{-2}] is shown in the fifth column, if available. A more comprehensive review is given by Bowyer (1990). The observed flux level in the present study is in a range of 300–600 CU. This is not so much different from the previously obtained value if the uncertainty in the absolute calibration and the difference in the observed area are taken into account. The isotropic component will be discussed in some detail in § 4.5.

4.3. *Model of the Scattered Light by High Galactic Latitude Dust Clouds*

We attempt to interpret the observed spatial variation of the FUV background radiation in terms of the light scattered by high Galactic latitude dust clouds. The basic observational data concerned are the relations given by equations (3), (4), (5), and (7).

4.3.1. *Dependence on the Galactic Latitude*

Jura (1979a) presented a simple model of light scattered by high Galactic latitude clouds. The Galaxy was assumed to be an infinite plane of uniform source and only the single scattering was taken into account. Jura (1979a) suggested that surface brightness S_λ of a cloud at a high latitude could be approximated within an accuracy of a factor of 1.5 by

$$S_\lambda = I_c\{1 - Q(\sin b)^{1/2}\}\,, \tag{10}$$

with

$$I_c = \frac{S_\lambda^0 \tau_\lambda a_\lambda}{2}\,,$$

and

$$Q = 1.1 g_\lambda\,,$$

TABLE 2

OBSERVATIONS OF DIFFUSE FUV RADIATION

Workers	Mode[a]	Region[b]	Variation[c]	Flux Level[d] (CU)	Isotropic Component[e] (CU)
Hayakawa et al. 1969	W	$0° \leq b \leq 40°$	L	1300	...
Lillie & Witt 1976	W	$\|b\| < 60°$	L, H I	1000	...
Morgan et al. 1978	W	$\|b\| < 36°$	L	...	...
Henry et al. 1978b	S	$\|b\| > 60°$	N	300	...
Pitz et al. 1979	W	$-20° < b < +82.5°$	N	2500	...
Anderson et al. 1979	S	$17° < b < 88°$	N	285 ± 32	...
Paresce et al. 1980	W	$\|b\| > 30°$	H I	$300 - 1000$	300
Zvereva et al. 1982	W	$-58° < b < +27°$	L, H I	700	...
Anderson et al. 1982	S	all b	N	<300	...
Weller 1983	W	NGP and SGP	...	$180 - 280$	...
Joubert et al. 1983	W	$\|b\| > 30°$	H I	$400 - 1200$	$300 - 690$
Jakobsen et al. 1984	W	$b \simeq 50°$	H I	$400 - 1600$	550 ± 150
Tennyson et al. 1988	S	$b \simeq 35°$	...	300 ± 100	...
Fix et al. 1989	W	$\|b\| < 60°$	L, H I	$300 - 800$	530 ± 80
Murthy et al. 1989	S	$-39° < b < 86°$	NS	700 ± 200	...
Murthy et al. 1990	S	$-39° < b < 86°$	NS	$300 - 900$	...
Hurwitz et al. 1990 (HMB)	S	$-39° < b < 88°$	L, H I	$350 - 500$	272 ± 13

[a] Observational mode: W, wide band photometry; S, spectrophotometry.

[b] Observed region. Only the Galactic latitude range is indicated. For the spectrophotometric observations, a small number of areas were observed.

[c] L, the latitude dependence is clearly seen; H I, the correlation with N(H I) is indicated; N, no variation is found; NS, the variation is found but not systematic.

[d] The flux level observed for the region of low N(H I) ($< 3 \times 10^{20}$ cm^{-2}), if available, in CU.

[e] The isotropic component suggested in CU, mostly derived from the intercept of the regression analysis with N(H I).

if we take the Henyey-Greenstein phase function as a scattering function and $b \geq 10°$, $g_\lambda \leq 0.8$, and $\tau_\lambda \leq 1$. Here S_λ^0 is the surface brightness of the Galactic disk, τ_λ is the optical depth of the cloud, a_λ is the albedo of the single scattering of the dust particle, and g_λ is the asymmetry factor of the phase function ($g_\lambda = 0$: isotropic scattering; $g_\lambda = +1$: complete forward-throwing scattering). For simplicity, the subscript λ is omitted for a and g of the FUV region in the following discussions.

The derived regression equation (3) for the present observation indicated, when the form of equation (10) is applied,

$$I_c = 3098.9 \pm 390.0 \quad \text{and} \quad Q = 0.9 \pm 0.1 \,. \qquad (11)$$

As pointed out in § 3.1, the fit of equation (3) is not very good and the scatter is larger than the observational errors. In applying simple models to the observed results in this section, we implicitly assume that the scatter comes from fluctuations of local physical conditions but the global characteristics are represented by equation (3). Thus, we assume that the average scattering properties of interstellar dust grains can be derived from the fit of equation (3) in the framework of the present analysis. In fact, numerical results of model calculation are well described by the functional form of $(\sin b)^{1/2}$.

There may be additional contributions from the uncorrected components in the observed data as discussed in the previous section. Summing up the possible contributions, we obtain 255 CU as an upper limit for the possible constant components other than the light scattered by dust. This gives about 7% increase in the parameter Q at most. There may exist the contribution from the extragalactic sources, which would further increase the value of Q. A simple comparison of the observed value of Q with equation (10) gives $g \approx 0.9 \pm 0.1$ or more. This is out of the range where the approximation is supposed to be valid and the simple use of equation (10) may be largely in error in this case.

We have repeated the calculation of Jura's (1979a) model and fitted the results with the form of equation (10) for the region $60° < b < 80°$. The numerical results showed that the dependence of Q on g becomes weak as g approaches to 1.0, and that Q is about 0.79 for $g = 0.9$. The value of Q does not exceed 0.8 even for $g = 0.99$. This is marginally compatible with the observationally derived value. This simple model analysis indicates a strongly forward-throwing scattering characteristics of the dust particles in any case.

The sky brightness due to stars in the FUV has been shown to be very anisotropic (Henry 1977; Gondhalekar, Phillips, & Wilson 1980; Henry, Anderson, & Fastie 1980). We relax the assumption of the uniform source distribution and examine the effects of the anisotropic distribution of the source. We use the empirical source distribution according to Gondhalekar et al. (1980). Details are given in the Appendix. If the anisotropy of the source distribution is taken into account, the surface brightness of the cloud must depend on the Galactic longitude l and the parameter Q becomes 0.85–0.89 for $g = 0.9$ and 0.75–0.82 even for $g = 0.5$ in the region $270° < l < 330°$, where the range of Q indicates the variation of the background radiation with l. The observed variation of the diffuse FUV radiation with l in the region of $1.8 \times 10^{20} < N(\text{H I}) < 2.0 \times 10^{20}$ cm^{-2} and $60° < b < 70°$ is shown in Figure 8. There is no noticeable systematic variation with l seen in this figure. The predicted variation with l increases as g increases and b decreases (see Appendix). As an example of the model which gives the largest variation, the model with $g = 0.9$ and $b = 60°$ is depicted by a broken line in Figure 8. The predicted variation is small and the refined model is roughly consistent with the observation as far as the variation with l is concerned for the restricted range of l observed. The analysis of the refined dust scattering model suggests that the observed latitude dependence requires an asymmetry factor of $g \geq 0.5$. This range of g is wider than that allowed for Jura's (1979a) model.

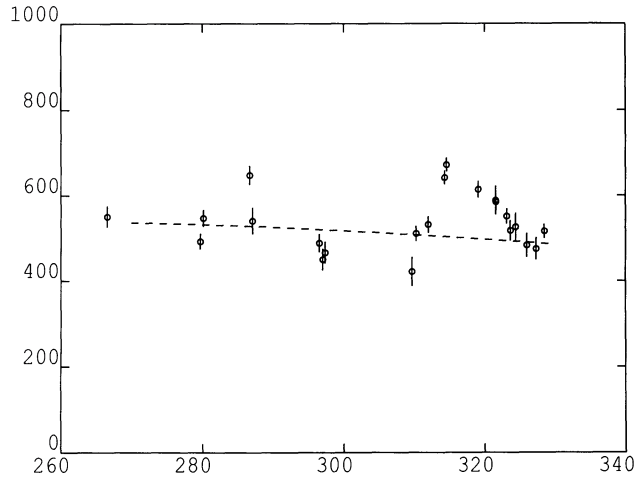

FIG. 8.—Variation of the diffuse FUV radiation (I_{FUV}) (photons cm^{-2} s^{-1} Å^{-1} sr^{-1}) with the Galactic longitude l (deg). Only the data in the range $60° < b < 70°$ and $1.8 \times 10^{20} < N(\text{H I}) < 2.0 \times 10^{20}$ cm^{-2} are plotted. A broken line indicates the result of the model calculation of $g = 0.9$ at $b = 60°$, taking account of the anisotropy of the source distribution.

The anisotropic distribution of the light source is, therefore, important in the study of the scattering light of the diffuse radiation. If observations cover a wide area, the longitudinal variation of the diffuse variation is expected and must be taken into account in the data analysis. The observations by Paresce et al. (1980) suggested a longitudinal variation, which may be consistent with the trend this model suggests (Fig. 9, in Appendix). The present model is, however, still very crude, and its validity must be confirmed by further observations covering over a wide field.

4.3.2. *Correlation with* H I

Figures 5 and 6 clearly indicate a correlation of the diffuse FUV radiation with N(H I) in the present data. Both correlations are roughly consistent, thus we take the relation given by equation (5) as a representative one in order to avoid the confusion with the variation dependent on b or l. The same refined model as employed in the previous subsection is applied. We found that the light scattered by high Galactic latitude dust clouds can be approximated by

$$I_{\text{FUV}}(\text{CU}) = 3680\tau_\lambda a(1 - 1.04g) \qquad (12)$$

for $270° < l < 330°$, $b > 70°$, and $g \geq 0$ with the accuracy of 20%. The optical depth of the dust cloud can be converted into the H I column density by using the relation

$$\tau_\lambda = \frac{1}{1.086} \frac{R_\lambda}{[N(\text{H I})/E(B-V)]} N(\text{H I}) , \qquad (13)$$

where R_λ is the normalized extinction [$= A_\lambda/E(B-V)$; A_λ, total extinction]. We take R_λ as 8.1 at 156 nm (Savage & Mathis 1979) and the gas-to-color excess ratio of N(H I)/$E(B-V)$ as 5.0×10^{21} atoms cm^{-2} mag^{-1} (Burstein & Heiles 1978). Knapp & Kerr (1974) obtained 5.1×10^{21} atoms cm^{-2} mag^{-1}, while Bohlin, Savage, & Drake (1978) derived 4.8×10^{21} atoms cm^{-2} mag^{-1} for H I alone. Thus, this value may be subject to an error of 2%–5%. There is an indication that the extinction curve in the high Galactic latitude region is slightly different from the standard one (Kiszkurno-Koziej & Lequeux 1987). The effect of the difference on R_λ is estimated to be 10%. Equation (13) with these values of the parameters leads to $\tau_\lambda < 0.45$ if $N(\text{H I}) < 3 \times 10^{20}$ cm^{-2}. The single scattering model is good enough for the analysis with the present accuracy of interest.

Substituting these values, we obtain from equations (12) and (13), and the slope of equation (5),

$$a(1 - 1.04g) = 0.18 \pm 0.03 . \qquad (14)$$

An upper limit of g is obtained, when $a = 1$, as 0.82. A lower limit of a can be placed, when g is taken as 0.5, the lowest possible value derived from the latitude dependence, to be 0.32. There may be some contributions from molecular hydrogen emission and line emission from the hot plasma to the observed slope, which was estimated to be less than 20% of the observed value (see §§ 4.1.5 and 4.2.6). This contribution would decrease the constant in the right-hand side of equation (14). Henry, Anderson, & Fastie (1980) reported the brightness of the Galactic disk in the range 120–170 nm, which was about 15% brighter than the brightness of the illuminating source adopted in the present study (Gondhalekar, Phillips, & Wilson 1980). If this correction of 15% is adopted, the constant of equation (14) will also decrease by the same fraction. Equation (14) does not include these systematic errors. Only the error in the regression analysis, which would be the same order as the systematic errors, is indicated. The correlation with N(H I) obtained in the present study indicates the relation between a and g as given by equation (14). Errors of equation (14) are estimated to be about 30%.

4.3.3. *Correlation with FIR*

According to Jakobsen et al. (1987), the far-infrared emission from the high Galactic latitude dust grain is given by

$$I_{\text{FIR}} = \frac{1}{2} \int_0^\infty I_\lambda^* \tau_\lambda (1 - a_\lambda) d\lambda , \qquad (15)$$

where I_λ^*, is the interstellar radiation. We do not have spectral information of a_λ in the FUV region, while the scattering properties of the interstellar dust grain are fairly well understood in the visual region (Witt 1989). As the first approximation to examine the constraint from FIR data, we divide the wavelength region into two parts: the FUV region [91.2 nm $< \lambda <$ 180 nm, where the albedo $a_\lambda (= a)$ is assumed to be constant] and the region of the wavelength longer than 180 nm. The boundary of 180 nm was taken rather arbitrarily. We fix it not to include the region of the intense 220 nm interstellar feature in the FUV region. The constancy of the albedo at wavelengths shorter than 180 nm is suggested recently by HMB. The parameter a is, in a sense, the albedo averaged over the FUV region with the interstellar radiation field (ISRF) (see below). In this model we do not take account of the anisotropy of the interstellar radiation field since the light absorption is not dependent on the direction from which the incident light comes unless the anisotropy in the dust shape distribution is prevailing.

We, then, rewrite equation (15) as

$$I_{\text{FIR}} = I_{\text{FIR}}(\text{FUV}) + I_{\text{FIR}}(\text{VIS-IR}) , \qquad (16)$$

with

$$I_{\text{FIR}}(\text{FUV}) = \frac{1}{2}(1 - a) \int_{91.2\text{ nm}}^{180\text{ nm}} I_\lambda^* \tau_\lambda d\lambda ,$$

$$I_{\text{FIR}}(\text{VIS-IR}) = \frac{1}{2} \int_{180\text{ nm}}^\infty I_\lambda^* \tau_\lambda (1 - a_\lambda) d\lambda .$$

We take the ISRF in the solar neighborhood of Mathis, Mezger, & Panagia (1983) except that we adopt the original data of Gondhalekar et al. (1980) rather than adjust it by 15% to match Henry et al. (1980) observations (Mezger, Mathis, & Panagia 1982) in order to have the consistency with the FUV scattering light model. We take the spectral dependence of dust optical depth of Cardelli, Clayton, & Mathis (1989) with $R_V = 3.1$ for $\lambda < 900$ nm and that of Martin & Whittet (1990) of the form of $\tau_\lambda \propto \lambda^{-1.8}$ for $\lambda > 900$ nm. The albedo around the 220 nm extinction hump is taken from Lille & Witt (1976), and a_λ is assumed to be 0.6 in the visual region (300 nm $< \lambda <$ 700 nm) (Witt 1989). In the wavelength region longer than 700 nm, the albedo calculated according to the interstellar dust model (Draine & Lee 1984) is assumed. Taking the same gas-to-color excess ratio adopted in § 4.3.2, we finally obtain

$$I_{\rm FIR}({\rm FUV}) = 7.1 \times 10^{-6}(1-a)\left[\frac{N({\rm H\ I})}{10^{20}\ {\rm cm}^{-2}}\right], \quad (17a)$$

$$I_{\rm FIR}({\rm VIS\text{-}IR}) = 1.39 \times 10^{-5}\left[\frac{N({\rm H\ I})}{10^{20}\ {\rm cm}^{-2}}\right], \quad (17b)$$

where $I_{\rm FIR}$(FUV) and $I_{\rm FIR}$(VIS-IR) are in the units of ergs cm^{-2} s^{-1} sr^{-1}. We find that about 60% of the energy absorption of $f_{\rm FIR}$(VIS-IR) occurs in the visual range (180 nm $< \lambda <$ 700 nm), and that there is almost negligible contribution to $f_{\rm FIR}$(VIS-IR) in $\lambda > 2$ μm. The contribution from the FUV region is about one-third even if $a = 0$.

The ISRF adopted is referred to the value in the solar neighborhood and the vertical dependence of the ISRF is neglected in the present study. Thus, the dust clouds are implicitly assumed to be located less than 1 kpc above the Galactic plane (Jura 1979a). The ISRF may have an accuracy of 15% in the overall spectrum (Mezger et al. 1982). The dust optical depth has been extensively studied recently and the accuracy should be rather high for the "standard interstellar extinction" ($R_V = 3.1$), in particular, in the visual region, where most absorption of the energy by dust particles occurs. The peculiar extinction suggested for the high Galactic region (Kiszkurno-Koziej & Lequeux 1987) adds an uncertainty of about 10% to equation (17a) as described in § 4.3.2. The accuracy of the albedo of the interstellar dust grain may be lower than that of the optical depth even in the visual region, being typically about 10% or less. Including all of these uncertainties, we estimate conservatively that the numerical factor in equations (17a) and (17b) may have an uncertainty of 50%.

In order to compare $f_{\rm FIR}$ with the flux at 100 μm, $f_\nu(100\ \mu{\rm m})$, the conversion suggested by Helou et al. (1988) is adopted:

$${\rm FIR} = 1.26 \times 10^{-5}[2.58 f_\nu(60\ \mu{\rm m}) + f_\nu(100\ \mu{\rm m})], \quad (18)$$

where FIR is in ergs cm^{-2} s^{-1} sr^{-1}, and $f_\nu(60\ \mu{\rm m})$ and $f_\nu(100\ \mu{\rm m})$ are the far-infrared fluxes obtained by *IRAS* in MJy sr^{-1}. Since no reliable value of $f_\nu(60\ \mu{\rm m})$ of the diffuse component is available in the present analysis, the ratio $f_\nu(60\ \mu{\rm m})/f_\nu(100\ \mu{\rm m}) = 0.29 \pm 0.05$ is taken from the study of the FIR emission in the north Galactic pole region by Boulanger & Pérault (1988). The parameter FIR estimates the flux contained between 42.5 and 122.5 μm within an accuracy of 1%, irrespective of the detailed shape of the emission. However, FIR does not include emission at shorter and longer wavelengths. The ratio of the total flux of a thermal source integrated between 1 to 1000 μm to FIR, q, depends on the shape of the dust opacity, ranging from 1.5 to 1.9 for the observed ratio of $f_\nu(60\ \mu{\rm m})/f_\nu(100\ \mu{\rm m})$ in a reasonable range of the dust opacities (Helou et al. 1988). We equalize simply the above estimated thermal emission to $I_{\rm FIR}$ to obtain

$$I_{\rm FIR} = (2.20 \pm 0.16) \times 10^{-5} q f_\nu(100\ \mu{\rm m}), \quad (19)$$

with $1.5 < q < 1.9$.

Combining equations (12) and (19), we obtain

$$\frac{I_{\rm FUV}}{f_\nu(100\ \mu{\rm m})} = (1701 \pm 124) q \frac{a(1-1.04g)}{(2.96-a)}. \quad (20)$$

From the observed relation given by equation (7), we find

$$a(1-1.04g) = (4.37 \pm 0.77) \times 10^{-2}(2.96-a)/q < 0.10. \quad (21)$$

Thus, even if the uncertainties are taken into account, equation (21) is marginally compatible with the relation given by equation (14) derived from the dependence of $I_{\rm FUV}$ on N(H I). Jakobsen et al. (1987) pointed out a similar discrepancy and discussed possible explanations. However, if we take the slope derived from the regression analysis between $f_\nu(100\ \mu{\rm m})$ and $I_{\rm FUV}$ with $I_{\rm FUV}$ being an independent variable instead of $f_\nu(100\ \mu{\rm m})$, the relation comes into the range consistent with equation (14).

Although the relation between $f_\nu(100\ \mu{\rm m})$ and $I_{\rm FUV}$ must be a direct one for the dust particles, we examine another relation between $f_\nu(100\ \mu{\rm m})$ and N(H I) in order to clarify this discrepancy in some more detail. In the north Galactic pole region, Boulanger & Pérault (1988) obtained

$$\left[\frac{f_\nu(100\ \mu{\rm m})}{{\rm MJy\ sr}^{-1}}\right] \propto (0.92 \pm 0.14)\left[\frac{N({\rm H\ I})}{10^{20}\ {\rm cm}^{-2}}\right], \quad (22)$$

where errors included the difference in the regression slopes derived by both $f_\nu(100\ \mu{\rm m})$ and N(H I) as independent variables. From this observational relation and equations (16), (17a), (17b), and (19), we obtain

$$(2.96-a) = (2.89 \pm 0.63) q > 3.4. \quad (23)$$

Even if $a = 0$, the absorbed energy is marginally consistent with the observed FIR flux within the uncertainties. Therefore, the discrepancy we found in equation (21) seems to originate from the *high FIR flux* compared to the available energy of ISRF rather than the observed low value of $I_{\rm FUV}$, if the standard gas-to-color excess ratio is applicable to the high Galactic latitude dust particles. The FIR observation, if it be correct, indicates that the albedo in the FUV region must be very small, and/or implies that the albedo in the visual to near-IR region may be lower than presently thought.

However, the latest observation by *COBE* showed that the diffuse FIR flux of *IRAS* was significantly higher than found by *DIRBE* experiment (Mather et al. 1990). The correction to the *IRAS* data is not straightforward, but at the ecliptic pole the surface brightness of *IRAS* is nearly 3 times higher than that of *DIRBE*. Thus, we must reserve the conclusion about the constraint imposed by the FIR data till the fully analyzed data of *COBE* become available. The total FIR radiation $I_{\rm FIR}$ should be able to be derived accurately from the data of *DIRBE* at 60, 100, 120–200, and 200–300 μm bands. If the albedo in the FUV region derived in the present study is correct ($a > 0.32$), we can predict the slope of the regression line of $I_{\rm FIR}$ versus N(H I) to be less than 1.9×10^{-5} ergs cm^{-2} s^{-1} sr^{-1} per 10^{20} cm^{-2} of N(H I).

4.4. *Scattering Properties of Dust Particles in the FUV*

The present study indicates a steep dependence of I_{FUV} on b and interprets it in terms of a strongly forward-throwing scattering of the interstellar dust grains in the FUV region ($g \geq 0.5$). A similar conclusion was reached by Henry (1981) and Anderson et al. (1982) from a different basis for the high Galactic latitude dust grains. The recent observation by Fix et al. (1989) also showed a steep dependence of the diffuse FUV radiation on b. They suggested a large value of g in the FUV, but their analysis is indicated to be incorrect because of the inappropriate omission of the optical depth term (Bowyer 1990).

On the other hand, observations of Galactic reflection nebulae and nebulosities indicate a trend of the scattering properties to become isotropic toward the FUV region in some case ($g \sim 0.2$) (Witt et al. 1982; Cardelli & Böhm 1984; Witt, Bohlin, & Stecher 1986) or a medium value of g in the FUV in another case ($g \approx 0.2$–0.6) (Onaka et al. 1984; de Boer & Kuss 1988). These results may indicate different populations between the dust particles in Galactic reflection nebulae and those in the interstellar space (Witt et al. 1986), while Chlewicki & Greenberg (1984b) pointed out the uncertainties associated with the model analysis of observations of reflection nebulae.

However, the latest spectroscopic observation of the diffuse FUV radiation by HMB indicates a highly isotropic scattering of the interstellar dust grains ($g \sim 0$) and a low albedo ($a \sim 0.2$) in the FUV region, which is incompatible with the present study. HMB obtained a low albedo value from the diffuse FUV radiation at low Galactic latitudes, which is supposed to be dependent on a but insensitive to g, and then derived a low value of g by comparing the correlation with N(H I) to the model calculation. In the present study, a large value of g was first suggested from the observed steep dependence of the diffuse FUV radiation on b and then a large value of a was obtained from the correlation with N(H I). In fact, if we take a small value of g (~ 0), equation (14) indicates $a \sim 0.2$, which is in agreement with the value of HMB. Thus, the discrepancy suggests that the diffuse FUV radiation observed at low Galactic latitude region and the observed steep dependence on b cannot be explained simply by the light scattering model with the same dust properties.

This may imply that the dust scattering properties or dust populations in low Galactic latitudes are not the same as those in high Galactic latitudes. As mentioned in § 4.3.2, there is some observational indication for the variation in dust population in high Galactic latitudes (Kiszkurno-Koziej & Lequeux 1987; Lequeux 1990; Witt 1990). Barsella et al. (1989) investigated the global motion of the interstellar dust grains in the Galaxy, implying a different population of dust grains in the high Galactic latitudes relative to low latitudes. This may resolve the discrepancy in the observations, but further observational works are needed to explore this hypothesis.

The present model does not take account of the vertical dependence of the ISRF and the multiple scattering, while the model by HMB includes these effects in order to account for the thick dust layer near the Galactic plane. The present model is applicable only to the diffuse radiation at high Galactic latitudes ($b > 40°$). The analysis of the present study indicates that the asymmetry of the light source distribution is important in the interpretation of the scattered light, in particular, in the high Galactic latitude region. The longitudinal effect must be investigated by further observations. More sophisticated models taking account of the radiative transfer effect are also needed for further detailed studies (Witt 1990).

The steep dependence of the diffuse FUV radiation on b seems to be secure because another observation by Fix et al. (1989) showed a similar trend clearly. Both observations are, however, wide band photometry. There might be contributions from unexpected components to the diffuse radiation, which can be distinguished only by the spectroscopic observation, although the estimates of possible components indicated their contribution not to be important (§ 4.1). If the subtraction of the stellar light is not properly done, a steep dependence on b may be expected. However, the contributions from faint stars is estimated not to be a strong function of b (§ 4.1.4). Further investigation may be needed to rule out the possibility of the Galactic faint star contribution to the background radiation to cause a steep latitude dependence.

Whether the albedo of the interstellar dust grains in the FUV region is high or low can in principle be determined by the observation of the diffuse FIR radiation. Since the fraction of the absorbed energy by dust grains in the FUV region may not be very large, the parameters involved in the interpretation of the FIR radiation must be fixed accurately enough. This kind of study may be a key to investigate the FUV scattering properties of the interstellar dust grains, but a clear conclusion from the FIR diffuse light must wait for the reliable *COBE* data to be available.

Theoretical model calculations of the interstellar grain model of Mathis, Rumpl, & Nordsieck (1977) indicate $g > 0.5$ and $a \sim 0.4$–0.5 in the FUV region (White 1979; Draine & Lee 1984). The values obtained in the present study are compatible to the range of these estimates. Chlewicki & Greenberg (1984a, b) theoretically investigated the UV scattering properties with a contribution from small grains as a parameter. They indicated $0.7 < g < 0.9$ and $a > 0.4$ in the FUV based on the consideration of the FUV extinction characteristics. These allowed ranges include the scattering parameters obtained in the present study, and a strongly forward-throwing scattering characteristics with high albedo ($a > 0.32$) would require a specific range of the parameters for the small dust grains. Detailed discussion of such models is out of scope of the present paper.

4.5. *Isotropic Component*

4.5.1. *Flux of Isotropic Component*

The isotropic component of the diffuse radiation is of great interest in relation to the extragalactic radiation. The flux of such a component is often derived from the intercept of the regression line with N(H I). However, as pointed out above, the intercept depends strongly on the slope estimated, and thus on the area which the observation covered. For instance, the regression line derived from the present observation of the wide area, equation (2), indicates a slow slope and an intercept of about 400 CU, while the regression analysis on the data of the Virgo cluster suggests a steep dependence and a small value of intercept of about 200 CU. According to the discussion above (§ 4.3), we believe that the slopes and the intercepts given by equations (4) and (5) represent a true dependence less affected by the anisotropy of spatial distribution of the diffuse radiation. We, therefore, conclude that the isotropic component in a standard sense is about 200–300 CU in the present observation.

While the value of the intercept is still dependent on the process of the data analysis, the observed flux level of 300–600

CU for $b > 70°$ and $N(\text{H I}) < 3 \times 10^{20}$ cm^{-2} can be straightly compared to previous observations. Table 2 indicates that the present flux level is in good agreement with recent observations, if the latitude dependence is taken into account. Henry et al. (1978b) presented the results of the observations of the north and south Galactic pole regions obtained by *Apollo 17* far-ultraviolet spectrometer (118–168 nm). They found a broad feature in the 140–150 nm region with the peak intensity of about 300 CU. A rocket-borne observation by Anderson et al. (1979) indicated the background radiation of 285 ± 32 CU in the 123 to 168 nm region and showed no spatial variation for $b > 65°$. Subtracting the line emissions mentioned above from the same data, Feldman et al. (1981) obtained the continuum background intensity of 150 ± 50 CU in the same range. Paresce et al. (1980) indicated that part of the observed FUV radiation obtained by *Apollo-Soyuz Test Project* is the Galactic origin, placing a strict upper limit to an extragalactic contribution of 300 CU. The background flux they observed was in the range 300–1000 CU for $N(\text{H I}) \leq 1 \times 10^{20}$ cm^{-2}, $330° < l < 30°$ and $30° < |b| < 70°$. Anderson et al. (1982) further analyzed the *Apollo 17* data, obtaining no significant residual intensity to a level of 300 CU between 118 and 168 nm. Weller (1983) reported the results of *Solad 11* satellite and presented 180 ± 75 CU at the north Galactic pole and 280 ± 88 CU at the south Galactic pole, interpreting them mostly as extragalactic origin. Based on the data by the *D2B-Aura* satellite, Joubert et al. (1983) showed that the best estimate for the true extragalactic background was in the range 300–690 CU at 169 nm. Their observed flux was in the range 400–1200 CU for $N(\text{H I}) < 2 \times 10^{20}$ cm^{-2} and $|b| > 30°$. Jakobsen et al. (1984) used a rocket-borne photometer, claiming an upper limit for the isotropic component at 159 nm to be 550 ± 150 CU with the flux range of 400–1600 CU at $b \sim 50°$. Holberg (1986) reported the results by *Voyager 2* UVS in the range 50 to 120 nm with the intensity of 100 to 200 CU in the region around the north Galactic pole. Tennyson et al. (1988) indicated a spectrally flat diffuse background radiation in the wavelength range 170 to 200 nm with the intensity of 300 ± 100 CU at a high Galactic latitude region by a rocket-borne spectrometer.

A latest experiment on board the Space Shuttle indicated the spectrally flat diffuse background radiation of 100 to 700 CU in the 120 to 170 nm region (Murthy et al. 1989) and 300 to 900 CU in 165 to 310 nm region (Murthy et al. 1990). Their results showed no correlation with H I column density, nor are they consistent with spatial isotropy. On the other hand, HMB indicated a clear dependence on b and concluded that a process associated with $N(\text{H I})$ produced most of the FUV continuum, and they showed an intensity of 350–500 CU for $|b| > 60°$. Fix et al. (1989) presented the recent observation by the imaging instrument on board the *Dynamic Explorer 1* satellite and reported that the background flux was in the range of 300–800 CU for $N(\text{H I}) < 3 \times 10^{20}$ cm^{-2} and that the isotropic component was deduced to be 530 ± 80 CU at 150 nm.

The radiation flux level of the present results (300–600 CU) may or may not be compatible with previous results. If the spatial variation is present but not very systematic, then the difference in the observed area must be taken into account in the comparison of the data. The intensity level of the present results is in good agreement with previous results at high Galactic latitudes ($b > 70°$). Observations at medium latitude ($b \sim 50°$–$60°$) resulted in a slightly stronger intensity range than the present results (e.g., Joubert et al. 1983; Jakobsen et al. 1984; Fix et al. 1989). If the dependence on the Galactic latitude we found is applicable to these data, the present results may not be incompatible with these medium-latitude observations.

The radiation flux of the isotropic component should involve several components discussed in § 4.1. If we sum up the estimates, we will get 140–150 CU (Table 1). We feel that this estimate is too conservative and there must remain residual components of more than 100 CU. HMB obtained the intercept to be 270 CU, including the two-photon emission. The value of the intercept of HMB itself is in good agreement of the present result. They further decomposed it from their spectroscopic data into the "true external" component and the light scattered by the dust grains in the warm ionized medium. The latter is supposed not to be correlated with $N(\text{H I})$. Since the present observation does not have spectral information, such a decomposition is not applicable. The best estimate of the isotropic component in the present study is 200–300 CU. This includes the contributions from various components discussed in § 4.1, the light scattered by dust grains not associated with $N(\text{H I})$, and the extragalactic component.

4.5.2. *Constraint on the Decay Time of a Heavy Neutrino*

De Rujula & Glashow (1980) suggested that the decay light from heavy neutrinos in the universe could be detected in the FUV background radiation. Maalampi, Mursula, & Roos (1986) derived a lifetime of the heavy neutrinos from the possible detection of the decay light based on the *IUE* observation. However, Murthy & Henry (1987) made careful examination on the same data and could not support the detection, and so far the decay light has not been confirmed. The upper limits of the detection provided lower limits of the lifetime of the heavy neutrinos (Kimble et al. 1981). Henry & Feldman (1981) pointed out that the search for the decay light in the massive objects, such as clusters of galaxies, could impose more stringent limits on the lifetime than the general FUV background radiation observations, and in fact they derived an improved lower limit from the observations of the Coma and the Virgo clusters from *Apollo 17* to be $1.1 \times 10^{25} h$ s for neutrino with mass around 15 eV c^{-2}, where h is the Hubble parameter in 100 km s^{-1} Mpc^{-1}. Holberg & Barber (1985) made analysis of the *Voyager 2* UVX observations of the Coma cluster, providing a lower limit of the lifetime for neutrinos of slightly larger mass (2.4×10^{25} to 7.1×10^{24} s for neutrino with mass of 22.1–27.8 eV c^{-2}).

The X-ray observations indicate that there is a large mass concentration in the center of the Virgo cluster (Fabricant & Gorenstein 1983), which is extended over the cluster size (Takano et al. 1989). The present observation does not have spectroscopic information for the radiation from the Virgo cluster and is not sensitive to the line emission, while the background radiations inside and outside the Virgo cluster were obtained and can be compared to investigate the excess diffuse radiation originating from the cluster. The background radiation outside the cluster to be compared was derived for the data averaged for $b > 70°$ and for $2.3 \times 10^{20} < N(\text{H I}) < 2.7 \times 10^{20}$ cm^{-2}, corresponding to the condition in the Virgo center.

We found that at the confidence level of 99% the difference between the outside background radiation and the diffuse radiation from the region within the radius of 1°.5 from the center of the Virgo cluster is less than 2 CU. If we take into account of a possible difference in the faint star contribution, which was

estimated to be less than 25 CU, we obtained from the sensitivity curve of GUV instrument that an upper limit of the FUV line emission around 150 nm, which may result from the neutrino decay, is 7700 photons cm^{-2} s^{-1} sr^{-1} as a conservative value. The X-ray observation indicates that the mass within the radius of 1°.5 is at least 8×10^{46} g, assuming that the distance to the Virgo cluster to be 15 Mpc (Fabricant & Gorenstein 1983). An upper limit to the decay light within 1°.5 radius is 20 photons cm^{-2} s^{-1}, and we obtain that a lower limit of the lifetime of the massive neutrinos is about 6×10^{24} s for the neutrino mass around 15 eV c^{-2}. If we relax the confidence level to 90%, a lower limit of 2×10^{25} s is obtained. This is a similar constraint to what Henry & Feldman (1981) claimed from the observation of the Virgo cluster as mentioned above. Their observation had a wider field of view (12° × 12°), giving an upper limit of the decay light of 180 photons cm^{-2} s^{-1} for much larger total mass neutrinos (1.2×10^{48} g).

5. SUMMARY

In this paper, we presented the diffuse background radiation obtained by a rocket-borne FUV imager around the Virgo cluster region. Contributions from several components other than the light scattered light by the interstellar dust grains were examined and found not to be dominant in the observed flux. From the observed flux, we obtained the following results:

1. The FUV background radiation showed a steep dependence on the Galactic latitude b.

2. A clear correlation of the background radiation with N(H I) was obtained if the observed region was restricted to $b > 70°$, indicating that a major fraction of the background radiation is Galactic origin.

3. The observed steep dependence on b can be explained by a simple model of light scattered by the interstellar dust grains if the anisotropy of the FUV source distribution is taken into account. This suggests that the anisotropic source distribution may be of great importance in the interpretation of the FUV background radiation. The validity of the present model must be confirmed by further observations.

4. The present model analysis indicated a medium to high albedo ($a \geq 0.32$) and a strongly forward-throwing scattering phase function ($g \geq 0.5$) for the interstellar dust grains in the FUV region. This is incompatible with HMB, who indicated a low albedo and an isotropic scattering in the FUV. The difference originates from the fact that the diffuse background flux at low Galactic latitudes ($10° < |b| < 20°$) found by HMB, and the steep dependence of flux on b cannot be simply explained by the simple model with the same dust properties both for high and low Galactic latitudes. Further investigations are needed to clarify the problem. The dust properties the present investigation indicated are in agreement with some theoretical predictions.

5. The isotropic component was estimated from the intercept of the regression line analysis with N(H I) to be 200 to 300 CU. This should include several components discussed in § 4.1 as well as the Galactic isotropic component and the true extragalactic component. Further decomposition would require spectroscopic information.

6. The difference in the background radiation between inside and outside the Virgo cluster region was found to be negligible. Assuming that the mass observed by X-ray in the Virgo cluster region is allocated to heavy neutrinos, no detection of the decay light indicates that a lower limit of the lifetime of the neutrino of the mass around 15 eV c^{-2} is 6×10^{24} s.

The authors wish to acknowledge their thanks to the experiment team of the GUV rocket observation for their cooperation, to the members of Prof. Okuda's laboratory at ISAS for providing the *IRAS* data and the information of the latest IR observations, to Charles F. Lillie for providing the latest results of the zodiacal light prior to publication, and to Carl Heiles for providing the H I 21 cm data of the Bell Laboratory. This study was partly supported by grant-in-aid 59065002 from the Ministry of Education, Science, and Culture.

APPENDIX

MODEL OF LIGHT SCATTERED BY HIGH GALACTIC LATITUDE DUST CLOUDS

Sandage (1976) discussed a simple model of the light scattered by high Galactic latitude dust clouds. Anderson et al. (1982) presented numerical results of a refined model. Jura (1979a) obtained a semi-analytical expression of the back-scattered light given by equation (10). Recently HMB investigated a detailed model, examining the effect of clumpy distribution of dust particles. In all of these models, the light source of the Galactic disk is assumed to be *uniform* in the longitudinal direction. Only in the study of HMB the dependence on the Galactic latitude and the vertical distribution of the radiation field are taken into account, while other models assume a uniform plane disk as a light source.

The prediction by Henry (1977) and observations by Gondhalekar et al. (1980) and Henry et al. (1980), however, revealed a highly asymmetric distribution of the sky brightness in the FUV region. To incorporate this asymmetric distribution into the model, we take the intensity I_λ^* at the Galactic disk as a function of l and b. The distribution was taken from the observational results by *TD-1* at 156.5 nm (Gondhalekar et al. 1980, Table 4). In the calculation, the difference in the absolute calibration between *TD-1* and GUV was taken into account (Paper I). The sky brightness of the *TD-1* data was multiplied by 0.8 so as to match with the GUV observation. Except for this modification, we take the same assumptions as Jura's (1979a) model: the scattering function of the dust particles is represented by the Henyey-Greenstein function and only the single scattering by dust in the cloud is taken into account.

Because we are based on the radiation field observed in the solar neighborhood, the model implicitly assumes that the location of the dust particles are not very high from the Galactic plane compared to the radial scale of the Galactic plane, being typically less than 1 kpc (Jura 1979a). On the other hand, we do not take account of the vertical dependence of I_λ^*. If the dust particles are located within the scale height of the FUV source stars (~100 pc), the dependence on b may become less steep. Because of other uncertainties involved in the model, we do not intend to refine further the model by taking account of the vertical dependence of the

TABLE 3

COEFFICIENTS OF MODEL APPROXIMATION

	Coefficients of Equation (A2)[a]			
g	d_1	d_2	e_1	e_2
0.0.....	0	0	0	4470
0.1.....	−1594	−893	1685	4969
0.2.....	−2956	−2157	3104	5731
0.3.....	−3993	−3424	4159	6454
0.4.....	−4596	−4358	4754	6787
0.5.....	−4683	−4731	4813	6604
0.6.....	−4251	−4467	4346	5834
0.7.....	−3389	−3646	3450	4575
0.8.....	−2268	−2474	2303	3032
0.9.....	−1084	−1191	1099	1442

[a] The coefficients of equation (A2) in CU for $b \geq 40°$.

source and the scattering clouds. In the present model, we examine the effects of the anisotropic distribution of I_λ^* to search for a possible explanation of the observed steep dependence of $I_{\rm FUV}$ on b.

Scattered light by a dust cloud at (l, b) was calculated for each g by integrating the contribution from the Galactic disk light source. The integration was made in the spherical coordinate and the divisions of the grids in the angle variables (θ and ϕ) are both 100. Models were calculated for the grids of 10° interval of l for $0° < l < 360°$ and 5° interval of b for $b \geq 40°$. Numerical results indicated that the scattered light distribution can be expressed approximately for the range $b \geq 40°$ by

$$I_{\rm sca} = c_1 \sin (l + 197°) + c_2 , \tag{A1}$$

where c_1 and c_2 are constants dependent on g. The strong light concentration at Gould's belt in FUV results in the sinusoidal dependence of the scattered light on l. We further fit the coefficients c_1 and c_2 by

$$c_i = d_i(\sin b)^{1/2} + e_i \qquad (i = 1, 2) \tag{A2}$$

for $b \geq 40°$. The approximation (A2) becomes worse as g increases, but the error is still about 11% even at $g = 0.9$. The coefficients d_i and e_i ($i = 1, 2$) are tabulated in Table 3 for $0 \leq g \leq 0.9$ in CU. The coefficients in equation (10), I_c and Q, can be calculated

$$I_c = e_1 \sin (l + 197°) + e_2 \tag{A3}$$

and

$$Q = [d_1 \sin (l + 197°) + d_2]/I_c . \tag{A4}$$

An example of the model with $g = 0.8$ is depicted in Figure 9. All of the estimation made in text refers to the approximation given by equation (A2) and the coefficients in Table 3.

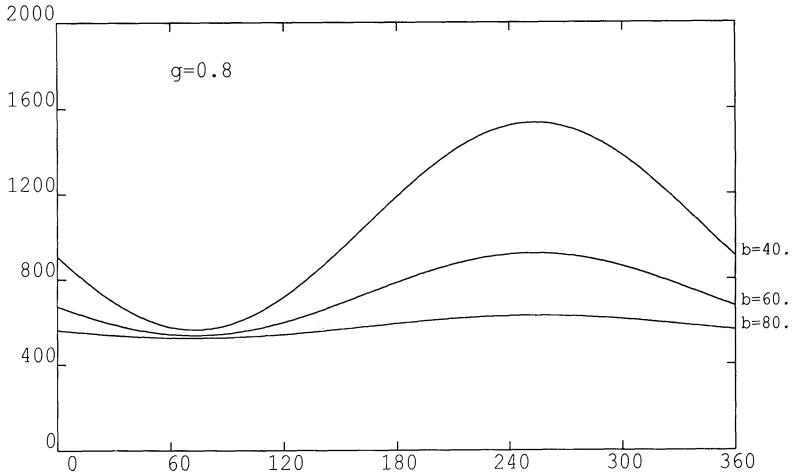

FIG. 9.—Examples of the model calculation of anisotropic source distribution, plotted as in Fig. 8. The longitudinal variations of the scattered light of the model with $g = 0.8$, $a = 1.0$, and $\tau = 1.0$ are shown for $b = 40°$, 60°, and 80°.

REFERENCES

Allen, C. W. 1973, Astrophysical Quantities (London: Athlone)
Anderson, R. C., Henry, R. C., & Fastie, W. G. 1982, ApJ, 259, 573
Anderson, R. C., Henry, R. C., Brune, W. H., Feldman, P. D., & Fastie, W. G. 1979, ApJ, 234, 415
Barsella, B., Ferrini, F., Greenberg, J. M., & Aiello, S. 1989, A&A, 209, 349
Bohlin, R. C., Hill, J. K., Stecher, T. P., & Witt, A. N. 1982, ApJ, 255, 87
Bohlin, R. C., Savage, B. D., & Drake, J. F. 1978, ApJ, 224, 132
Bowyer, S. 1990, in IAU Symposium 139, Galactic and Extragalactic Background Radiation, ed. S. Bowyer & Ch. Leinert (Dordrecht: Kluwer), 171
Boulanger, F., & Pérault, M. 1988, ApJ, 330, 964
Burstein, D., & Heiles, C. 1978, ApJ, 225, 40
Brune, W. H., Feldman, P. D., Anderson, R. C., Fastie, W. G., & Henry, R. C. 1978, Geophys. Res. Letters, 5, 383
Cardelli, J. A., & Böhm, K.-H. 1984, ApJ, 285, 613
Cardelli, J. A., Clayton, G. C., & Mathis, J. S. 1989, ApJ, 345, 245
Carruthers, G. R., & Opal, C. B. 1977a, ApJ, 212, L27
———. 1977b, ApJ, 217, 95
Chlewicki, G., & Greenberg, J. M. 1984a, MNRAS, 210, 791
———. 1984b, MNRAS, 211, 719
Code, A. D., & Welch, G. A. 1982, ApJ, 256, 1
Cowsik, R., & McClelland, J. 1972, Phys. Rev. Letters, 29, 669
Cox, P., & Leene, A. 1987, A&A, 174, 203
de Boer, K., & Kuss, C. 1988, A&A, 203, 149
Deharveng, J., Joubert, M., & Barge, P. 1982, A&A, 109, 179
De Rujula, A., & Glashow, S. L. 1980, Phys. Rev. Letters, 45, 942
Désert, F. X., Bazell, D., & Boulanger, F. 1988, ApJ, 334, 815
Draine, B. T., & Lee, H. M. 1984, ApJ, 285, 89
Duley, W. W., & Williams, D. A. 1980, ApJ, 242, L179
Fabricant, D., & Gorenstein, P. 1983, ApJ, 267, 535
Feldman, P. D., Brune, W. H., & Henry, R. C. 1981, ApJ, 249, L51
Fix, J. D., Craven, J. D., & Frank, L. A. 1989, ApJ, 345, 203
Giovanelli, R., & Haynes, M. P. 1989, ApJ, 346, L5
Gondhalekar, P. M., Phillips, A. P., & Wilson, R. 1980, A&A, 85, 272
Hayakawa, S., Yamashita, K., & Yoshioka, S. 1969, Ap&SS, 5, 493
Heiles, C. 1975, A&AS, 20, 37
Heiles, C., Stark, A. A., & Kulkarni, S. 1981, ApJ, 247, L73
Helou, G., Khan, I. R., Malek, L., & Boehmer, L. 1988, ApJS, 68, 151
Henry, R. C. 1977, ApJS, 33, 451
———. 1981, ApJ, 244, L69
Henry, R. C., Anderson, R. C., & Fastie, W. G. 1980, ApJ, 239, 859
Henry, R. C., Anderson, R., Feldman, P. D., & Fastie, W. G. 1978a, ApJ, 222, 902
Henry, R. C., & Feldman, P. D. 1981, Phys. Rev. Letters, 47, 618
Henry, R. C., Feldman, P. D., Fastie, W. G., & Weinstein, A. 1978b, ApJ, 223, 437
Holberg, J. B. 1986, ApJ, 311, 969
Holberg, J. B., & Barber, H. B. 1985, ApJ, 292, 16
Hurwitz, M., Martin, C., & Bowyer, S. 1990, ApJ, submitted (HMB)
Ionospheric Data in Japan 1987, Vol. 39, No. 2 (Radio Research Laboratory, Japan, Tokyo)
IRAS Explanatory Supplement 1986, ed. C. A. Beichman, G. Neugebauer, H. J. Habing, P. E. Clegg, & T. J. Chester (Washington, DC: GPO)
Jaccia, L. G. 1977, Smithsonian Ap. Obs. Spec. Rept., No. 375
Jakobsen, P. 1982, A&A, 106, 375
Jakobsen, P., Bowyer, S., Kimble, R., Jelinsky, P., Grewing, M., Krämer, G., & Wulf-Mathies, C. 1984, A&A, 139, 481
Jakobsen, P., de Vries, J. S., & Paresce, F. 1987, A&A, 183, 335
Joubert, M., Masnou, J. L., Lequeux, J., Deharveng, J. M., & Cruvellier, P. 1983, A&A, 128, 114
Jura, M. 1975, ApJ, 197, 575
———. 1979a, ApJ, 227, 798
———. 1979b, ApJ, 231, 732
Kimble, R., Bowyer, S., & Jakobsen, P. 1981, Phys. Rev. Letters, 46, 80
Kiszkurno-Koziej, E., & Lequeux, J. 1987, A&A, 185, 291
Knapp, G. R., & Kerr, F. J. 1974, A&A, 35, 361
Kodaira, K., Watanabe, T., Onaka, T., & Tanaka, W. 1990, ApJ, 363, 422 (Paper II)
Lequeux, J. 1990, in IAU Symposium 139, Galactic and Extragalactic Background Radiation, ed. S. Bowyer & Ch. Leinert (Dordrecht: Kluwer), 185
Lillie, C. F. 1990, in IAU Colloquium 126, Origin and Evolution of Interplanetary Dust (Tokyo: Kluwer), in press
Lillie, C. F., & Witt, A. N. 1976, ApJ, 208, 64
Maalampi, J., Mursula, K., & Roos, M. 1986, Phys. Rev. Letters, 56, 1031
Mather, J. C., et al. 1990, *COBE* preprint
Martin, C., & Bowyer, S. 1989, ApJ, 338, 677
———. 1990, ApJ, 350, 242
Martin, C., Hurwitz, M., & Bowyer, S. 1990, ApJ, 354, 220
Martin, P. G., & Whittet, D. C. B. 1990, ApJ, 357, 113
Mathis, J. S., Mezger, P. G., & Panagia, N. 1983, A&A, 128, 212
Mathis, J. S., Rumpl, W., & Nordsieck, K. H. 1977, ApJ, 217, 425
Mezger, P. G., Mathis, J. S., & Panagia, N. 1982, A&A, 105, 372
Morgan, D. H., Nandy, K., & Thompson, G. I. 1978, MNRAS, 185, 371
Murthy, J., & Henry, R. C. 1987, Phys. Rev. Letters, 58, 1581
Murthy, J., Henry, R. C., Feldman, P. D., & Tennyson, P. D. 1989, ApJ, 336, 954
———. 1990, A&A, 231, 187
O'Connell, R. W. 1987, AJ, 94, 876
Onaka, T. 1990, in IAU Symposium 139, Galactic and Extragalactic Background Radiation, ed. S. Bowyer & Ch. Leinert (Dordrecht: Kluwer), 379
Onaka, T., Sawamura, M., Tanaka, W., & Ogawa, T. 1985, Ap&SS, 114, 387
Onaka, T., Sawamura, M., Tanaka, W., Watanabe, T., & Kodaira, K. 1984, ApJ, 287, 359
Onaka, T., et al. 1989, ApJ, 342, 238 (Paper I)
Paresce, F. 1990, in IAU Symposium 139, Galactic and Extragalactic Background Radiation, ed. S. Bowyer & Ch. Leinert (Dordrecht: Kluwer), 307
Paresce, F., & Jakobsen, P. 1980, Nature, 288, 119
Paresce, F., Margon, B., Bowyer, S., & Lampton, M. 1979, ApJ, 230, 304
Paresce, F., McKee, C., & Bowyer, S. 1980, ApJ, 240, 387
Pitz, E., Leinert, C., Schulz, A., & Link, H. 1979, A&A, 72, 92
Reynolds, R. J. 1984, ApJ, 282, 191
———. 1990, in IAU Symposium 139, Galactic and Extragalactic Background Radiation, ed. S. Bowyer & Ch. Leinert (Dordrecht: Kluwer), 157
Rusch, D. W., & Sharp, W. E. 1981, J. Geophys. Res., 86, 10111
Sandage, A. 1976, AJ, 81, 954
Savage, B. D., & Mathis, J. S. 1979, ARA&A, 17, 73
Severny, A. B., & Zvereva, A. M. 1983, Ap. Letters, 23, 71
Stark, A. A., Bally, J., Linke, R. A., & Heiles, C. 1990, in preparation
Sternberg, A. 1989, ApJ, 347, 863
Takano, S., Awaki, H., Koyama, K., Kunieda, H., Tawara, Y., Yamauchi, S., Makishima, K., & Ohashi, T. 1989, Nature, 340, 289
Tennyson, P. D., Henry, R. C., Feldman, P. D., & Hartig, G. F. 1986, J. Geophys. Res., 91, 10141
———. 1988, ApJ, 330, 435
Thompson, G. L., Nandy, K., Jamar, C., Monfils, A., Houziaux, L., Carnochan, D. J., & Wilson, R. 1978, Catalogue of Stellar Ultraviolet Fluxes (Science Research Council)
Weller, C. S. 1983, ApJ, 268, 899
Wesselius, P. R., van Duinen, R. J., Aalders, J. W. G., & Kester, D. 1980, A&A, 85, 221
Wesselius, P. R., van Duinen, R. J., de Jonge, A. R., Aalders, J. W. G., Luinge, W., & Wildeman, K. J. 1982, A&AS, 49, 427
White, R. L. 1979, ApJ, 229, 954
Witt, A. N. 1989, in IAU Symposium 135, Interstellar Dust, ed. L. J. Allamandola & A. G. G. M. Tielens (Dordrecht: Kluwer), 87
———. 1990, in IAU Symposium 139, Galactic and Extragalactic Background Radiation, ed. S. Bowyer & Ch. Leinert (Dordrecht: Kluwer), 127
Witt, A. N., Bohlin, R. C., & Stecher, T. P. 1986, ApJ, 302, 421
Witt, A. N., Walker, G. A. H., Bohlin, R. C., & Stecher, T. P. 1982, ApJ, 261, 492
Zvereva, A. M., Severny, A. B., Granitzky, L. V., Hua, C. T., Cruvellier, P., & Courtès, G. 1982, A&A, 116, 312